Quantum-Dot Spin Chains

John M. Nichol

Abstract Semiconductor quantum dots are a promising platform for quantum simulation and computing. This chapter will review the fundamentals of semiconductor quantum dots and the Heisenberg exchange coupling that occurs between neighboring quantum dots. Despite directly coupling only nearest-neighbor quantum dots, exchange coupling underlies a great many approaches for quantum information processing, quantum state transfer, and the simulation of spin chain dynamics. This chapter will review recent progress and future work along these directions.

1 Introduction

Semiconductor quantum dots are three-dimensional confining potentials for electrons. They enable trapping, manipulating, and measuring the charge and spin states of single electrons in semiconductors. As a result of these capabilities, semiconductor quantum dots are a leading platform for quantum computing and simulation. A unique feature of electrons in semiconductor quantum dots is Heisenberg exchange coupling between neighboring electrons, which results from the interplay of the Pauli exclusion principle, the electrostatic confinement potential, the Coulomb interaction between electrons, and the external magnetic field. The possibility of

This work was sponsored by the Defense Advanced Research Projects Agency under grant D18AC00025; the Army Research Office under grants W911NF-17-1-0260 and W911NF-19-1-0167; the National Science Foundation under grants DMR-1809343, DMR 2003287, and OMA 1936250; and the Office of Naval Research under grant N00014-20-1-2424. The views and conclusions contained in this document are those of the authors and should not be interpreted as representing the official policies, either expressed or implied, of the Army Research Office or the U.S. Government. The U.S. Government is authorized to reproduce and distribute reprints for government purposes notwithstanding any copyright notation herein.

J. M. Nichol (✉)
Department of Physics and Astronomy, University of Rochester, Rochester, NY, USA
e-mail: john.nichol@rochester.edu

A. Bayat et al. (eds.), *Entanglement in Spin Chains*, Quantum Science and Technology, https://doi.org/10.1007/978-3-031-03998-0_17

exchange coupling between electrons together with the capabilities of single-charge and single-spin control and readout means that semiconductor quantum dots offer a natural environment in which to explore both tunnel-coupled and exchange-coupled spin chains. Indeed, significant progress has been made in recent years in simulating and exploring different aspects of the Hubbard and Heisenberg models in quantum-dot spin chains, finally bringing to fruition several decades of previous theoretical work.

This chapter will describe recent progress in this field. We begin with an overview of gate-defined semiconductor quantum dots and how they work. We then describe the origins of exchange coupling in quantum-dot spin chains and some of the many uses of exchange coupling in quantum computing with semiconductor spin qubits. Then, we discuss recent advances in the experimental realization and exploration of quantum-dot spin chains, including simulation of the Hubbard model and the Heisenberg model. A recurring theme in this chapter is that technological advances driven primarily by potential applications in quantum computing have also created new opportunities in quantum simulation. In turn, advances in quantum simulation have also enabled new capabilities for quantum computing. A notable example is that the studies of Hubbard and Heisenberg physics in quantum-dot spin chains have enabled advances in methods for quantum state transfer in spin chains, which are beneficial for quantum computing.

The experimental and theoretical development of quantum-dot spin chains has remained an active area of research for several decades at institutions around the world. The interested reader is encouraged to consult the references herein for further information. Portions of this chapter are reprinted from Kandel et al., App. Phys. Lett., 119, 030501 (2021) with the permission of AIP Publishing.

2 Gate-Defined Quantum Dots

Although different experimental platforms exist that feature exchange coupling [2, 3], and although different types of quantum dots exist, this chapter focuses on gate-defined quantum dots in semiconductors [4–8], one of the most promising systems for the creation and exploration of spin chains. In this section, we will discuss the basic operation of quantum dots, how tunneling and exchange coupling can occur in quantum dots, and experimental demonstrations of exchange.

2.1 Quantum-Dot Fabrication

Gate-defined quantum dots are usually created using a layered semiconductor heterostructure, such as GaAs/AlGaAs, Si/SiGe, Si/SiO_2, or Ge/SiGe [4–10]. Such heterostructures are often grown by advanced material growth techniques, like molecular beam epitaxy or chemical vapor deposition. A common feature of all

of these material platforms is that they enable the creation and control of two-dimensional electron or hole systems, called two-dimensional electron (or hole) gasses. In GaAs/AlGaAs and Si/SiO_2 systems, electrons are confined to the interface between two materials, while in Si/SiGe or Ge/SiGe quantum wells, the electrons or holes are confined within a thin semiconductor layer, called a "quantum well." In all cases, the confinement is enabled by the band gap mismatch between the various materials involved, and the two-dimensional electron or hole system typically resides within tens of nanometers of the semiconductor surface. Lithographically defined metal wires, or "gates," are typically fabricated on top of the heterostructure. Voltages applied to these gates generate electrostatic potentials that fully confine the electrons. The magnitude and sign of the voltages depend on the details of the heterostructure and device design. For example, GaAs/AlGaAs heterostructures usually feature a layer of Si dopants in the heterostructure to create a nonzero density of electrons in the two-dimensional electron gas without any applied voltages to the gates. Therefore, to create electrostatic confinement, negative voltages are applied to the gates to "deplete" various regions of the two-dimensional electron gas. Heterostructures based on Si are typically undoped, and positive voltages must generally be applied to the gates to "accumulate" electrons. In addition to the dots themselves, the gates can also define electronic reservoirs, from which the dots are loaded or unloaded, and tunnel barriers between dots or between dots and reservoirs. Figure 1 illustrates typical quantum-dot designs.

The growth, characterization, and optimization of two-dimensional electron or hole systems are the focus of significant research worldwide. The development of high-quality Si/SiO_2 transistors underlies the modern microelectronics industry. Si/SiGe and Ge/SiGe quantum wells are also the focus of significant development for transistor applications, and GaAs/AlGaAs heterostructures find significant use in optical and solar applications. The development of quantum-dot spin qubits and related systems has thus benefited tremendously from advances in the fabrication of semiconductor devices.

Early gate-defined quantum dots were fabricated in GaAs/AlGaAs heterostructures [4–8]. This material features extremely high electron mobilities and correspondingly long mean free paths. (Gate-defined quantum dots cannot usually be formed in materials with low mobilities, because the associated strong disorder typically means that electrons will localize around defect sites instead of the desired electrostatic potential.) However, all nuclear isotopes of Ga and As have nuclear spin $I = 3/2$. These nuclear spins generate an effective magnetic field experienced by electrons in the quantum dots through the hyperfine interaction [11]. On the one hand, hyperfine fields generally increase dephasing rates and decrease coherence times of electrons [11]. On the other hand, nuclear spins can create a convenient source of magnetic disorder [12], which is potentially useful for quantum simulation, as discussed further below.

Si/SiGe and Ge/SiGe quantum wells and Si/SiO_2 systems partly solve the challenge of hyperfine fields because both Si and Ge can be isotopically purified to select isotopes with zero nuclear spin [9]. However, Si two-dimensional electron systems generally feature larger conduction band effective masses than carriers in

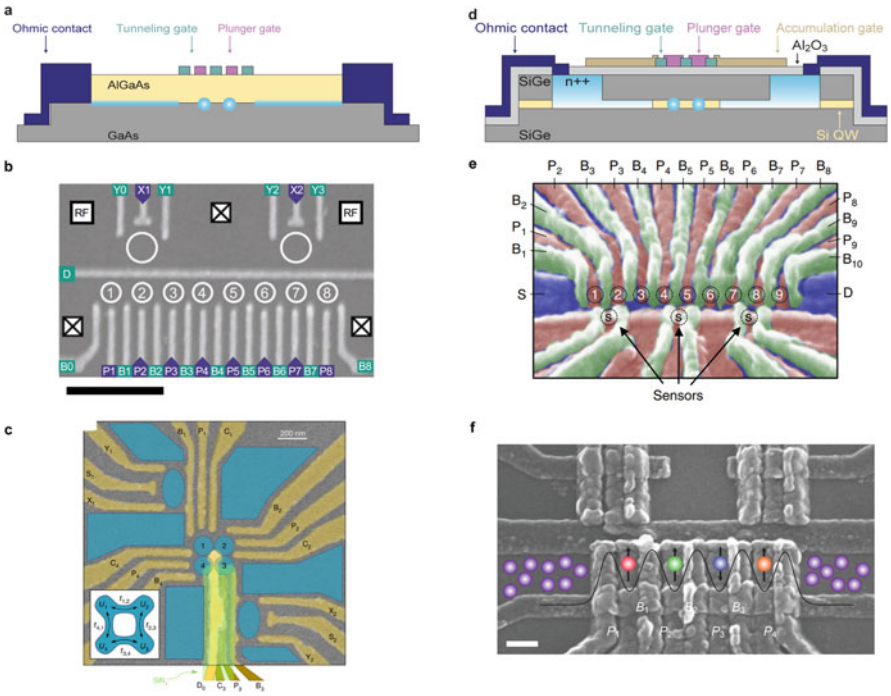

Fig. 1 Quantum-dot spin chains. (**a**) Schematic of a typical depletion-mode quantum-dot device in GaAs. Electrons from metal Ohmic contacts populate the two-dimensional electron gas (light blue) and are confined with tunneling and plunger gates. (**b**) Eight-quantum-dot linear array in GaAs, Volk et al., Nat. Comm., 5, 29 (2019). Copyright the Authors, licensed under a Creative Commons Attribution (CC BY) license. (**c**) Four-quantum-dot square array in GaAs/AlGaAs. Reprinted with permission from Deholain et al., Nature, 579, 528–533 (2020). Copyright Springer Nature (2020). (**d**) Schematic of a typical overlapping-gate device in Si/SiGe. Here, positive voltages applied to accumulation gates define the electronic reservoirs. (**e**) Nine-dot linear array in Si/SiGe. Mills et al., Nat. Comm., 10, 1063 (2019). Copyright the Authors, licensed under a Creative Commons Attribution (CC BY) license. (**f**) Four-dot linear array with the overlapping gate architecture in GaAs/AlGaAs. Reprinted from Kandel et al., App. Phys. Lett., 119, 030501 (2021) with the permission of AIP Publishing. In all panels, circles denote the locations of the electrons

GaAs/AlGaAs. Because orbital energy splittings generally scale inversely with the effective mass of the carriers, typical quantum dots in Si must be smaller than GaAs dots to compensate for the increased effective mass. An additional complication results from the fact that Si is an indirect gap semiconductor, and there are multiple equivalent valleys in the conduction band near the edges of the Brilluoin zone [9]. Thus, electrons in Si quantum dots have an additional valley degree of freedom that must typically be accounted for. Germanium quantum wells, which support two-dimensional hole systems can potentially overcome these two obstacles, with relatively small effective masses and a valence band maximum at the center of the Brillouin zone, eliminating the valley degeneracy of Si systems [10]. In the

following, we will primarily discuss quantum-dot spin chains in the context of electrons in GaAs- and Si-based systems, because most of the advances have occurred in these material platforms. The exploration of spin chains in Ge/SiGe systems is an exciting prospect for future work.

2.2 Quantum-Dot Operation

Individual quantum dots are typically operated at cryogenic temperatures, where the thermal energy of the environment is much less than the charging energy (the energy to overcome the Coulomb repulsion and add another electron to the dot) and the orbital energy spacings of the quantum dots. In such a regime, quantum dots are frequently connected via tunnel barriers to source and drain reservoirs, which are held at fixed potential via galvanic contacts to external voltage sources. The physics of electrons in quantum dots is reviewed in Refs. [4–8], and the interested reader is encouraged to consult these references.

When the electrochemical potential of a quantum-dot state lies between the electrochemical potential of the source and drain reservoirs, current can flow through the quantum dot, as a result of tunneling from the source, through the dot, and into the drain. When the electrochemical potential of the dot is not between those of the source and drain reservoirs, the current flow is blocked, and the dot is the Coulomb blockade regime. By tuning the gate voltages to be less positive or more negative, the number of electrons in the dot reduces, until all electrons are gone, resulting in no further current peaks. Thus, the Coulomb blockade allows one to concretely identify the number of electrons in a quantum dot. The detection of quantum-dot charge states most often relies on a proximal charge sensor, such as a quantum point contact or quantum dot, whose electrical conductance depends sensitively on local electric fields, including those from nearby charged quantum dots [16–19]. Quantum dots may be tunnel coupled, usually in series, between reservoirs [6]. A prototypical example is a double quantum dot, with two dots coupled in series between two reservoirs.

Many studies of individual and few quantum-dot systems have occurred over the last several decades, leading to significant advances in quantum information processing with semiconductor quantum dots [20]. As spin-based quantum information processors scale up, a primary challenge in creating many-qubit systems is the difficulty in "tuning up" devices with many quantum dots. Typically, an experimenter must spend time tuning the gate voltages to achieve the right potential landscape. A major difficulty in achieving the proper potential for many dots simultaneously is the effect of defects in the semiconductor. Indeed, a major effort in the development of quantum dots in recent decades has been to improve the tunability of the potential landscape to overcome this challenge. For example, the first quantum dots used a vertical architecture, in which the parameters of the confinement potential were set by the growth of the heterostructure [21, 22]. To promote better in-situ tunability, early lateral quantum dots featured a "stadium-style" architecture [23], in which

electric fields from nearby metal gates create the confinement potential (Fig. 1a–c). Such an architecture features significantly improved tunability over earlier vertical architectures. Recently, a new generation of quantum dots with an "overlapping-gate" architecture has emerged [24–26] (Fig. 1d–f). In contrast to the stadium-style architecture, the overlapping-gate architecture involves voltages applied to gates directly above the quantum-dot location. These devices feature strong electrostatic confinement and tight control over nearly all of the relevant parameters of the quantum-dot confinement. Additional advances that have enabled the creation of extended spin chains are various procedures for computer automated tuning and independent control of the quantum-dot potential parameters [27–35].

2.3 Exchange Coupling in Quantum Dots

Electrons are fermions. Thus, according to the Pauli exclusion principle, no two electrons can have the same quantum numbers. In nanoscale quantum systems, a direct manifestation of the Pauli exclusion principle is the Heisenberg exchange coupling between two electrons $H = J\mathbf{S}_1 \cdot \mathbf{S}_2 - 1/4$, where $\mathbf{S}_1$ and $\mathbf{S}_2$ are spin-1/2 operators associated with the spins of the two electrons [36–38].

Although a detailed calculation of the exchange coupling J presents a substantial challenge, the following heuristic picture illuminates the mechanism behind exchange coupling in semiconductor quantum dots. Consider two electrons in a single quantum dot. The overall wavefunction of the two electrons must be antisymmetric under particle exchange. If the two electrons occupy the spin singlet state $|S\rangle = \frac{1}{\sqrt{2}}(|\uparrow\downarrow\rangle - |\downarrow\uparrow\rangle)$, the spin component of the wavefunction is antisymmetric under exchange. Therefore, the orbital part of the wavefunction must be symmetric in order to guarantee that the overall wavefunction is antisymmetric under exchange. In particular, both electrons can occupy the ground state orbital of the quantum dot. Similarly, if the two electrons have any of the triplet states $\{|T_0\rangle = \frac{1}{\sqrt{2}}(|\uparrow\downarrow\rangle + |\downarrow\uparrow\rangle), |T_-\rangle = |\downarrow\downarrow\rangle, |T_+\rangle = |\uparrow\uparrow\rangle\}$, the electrons must have an antisymmetric orbital wavefunction to guarantee the overall antisymmetry of the total wavefunction. In particular, both electrons cannot occupy the ground state orbital of the quantum dot, and the triplet states will have a higher energy than the singlet. The energy splitting between the singlet and triplet states is the exchange coupling energy.

The phrase "Pauli spin blockade" is also used to describe a related phenomenon. Similar to the Coulomb blockade, where the presence of an electron in a quantum dot prevents the addition of further electrons until the Coulomb repulsion is overcome, the Pauli spin blockade describes a scenario in which the presence of a spin in a quantum dot prevents the addition of another spin in a symmetric spin configuration until the exchange energy can be overcome.

It is straightforward to show that the singlets and triplets are eigenstates of the Heisenberg Hamiltonian discussed above, and when $J > 0$, the singlet has a lower energy than the triplets. To understand some of the important physical mechanisms

underlying exchange coupling, let us consider the following Hubbard model for electrons in N quantum dots:

$$H_{Hub} = \sum_{i=1}^{N} \left[\frac{\tilde{U}}{2} n_i (n_i - 1) + V_i n_i \right] + \sum_{\langle i,j \rangle} U_C n_i n_j + \sum_{\langle i,j \rangle} t \sum_{\sigma=\uparrow\downarrow} (c_{i,\sigma}^{\dagger} c_{j,\sigma} + \text{h.c.}). \tag{1}$$

Here, $c_{i,\sigma}^{\dagger}$ is a fermionic operator that creates an electron in dot i with spin σ, and $n_i = \sum_\sigma c_{i,\sigma} c_{i,\sigma}^{\dagger}$ is the number operator for dot i. V_i is the gate-controlled energy of dot i, $\tilde{U}$ is the on-site Coulomb energy, U_C is the nearest-neighbor Coulomb energy, $\langle i, j \rangle$ indicates a sum over nearest neighbors, and t is the hopping energy between dots. It can be shown that when the number of electrons in the system is the same as the number of quantum dots, this Hamiltonian can be transformed to the Heisenberg Hamiltonian in certain parameter regimes [39].

To see how exchange coupling can occur in the Hubbard model, we consider two electrons in a double quantum dot, and we consider the matrix elements of this Hamiltonian in the following basis:

$$|T_0(1,1)\rangle = \frac{1}{\sqrt{2}} (c_{1,\uparrow}^{\dagger} c_{2,\downarrow}^{\dagger} + c_{1,\downarrow}^{\dagger} c_{2,\uparrow}^{\dagger}) |0\rangle \tag{2}$$

$$|S(1,1)\rangle = \frac{1}{\sqrt{2}} (c_{1,\uparrow}^{\dagger} c_{2,\downarrow}^{\dagger} - c_{1,\downarrow}^{\dagger} c_{2,\uparrow}^{\dagger}) |0\rangle \tag{3}$$

$$|S(2,0)\rangle = c_{1,\uparrow}^{\dagger} c_{1,\downarrow}^{\dagger} |0\rangle \tag{4}$$

$$|S(0,2)\rangle = c_{2,\uparrow}^{\dagger} c_{2,\downarrow}^{\dagger} |0\rangle , \tag{5}$$

where $|0\rangle$ indicates the state with no electrons, and the numbers in parentheses give the numbers of the electrons in both quantum dots. In this basis, the Hubbard Hamiltonian has the following form:

$$H_{Hub} = \begin{pmatrix} 0 & 0 & 0 & 0 \\ 0 & 0 & \sqrt{2}t & \sqrt{2}t \\ 0 & \sqrt{2}t & U + \epsilon' & 0 \\ 0 & \sqrt{2}t & 0 & U - \epsilon' \end{pmatrix}, \tag{6}$$

up to an overall energy shift, and where $U = \tilde{U} - U_C$, and $\epsilon' = V_1 - V_2$. Below, we refer to ϵ' as the detuning of the double quantum dot. We set $\epsilon = U + \epsilon'$ [i.e., we set the zero of the detuning to the (1,1)-(2,0) charge transition], and then we diagonalize the subspace spanned by $|S(1,1)\rangle$ and $|S(2,0)\rangle$ to give new effective singlet states $|S_-\rangle$ and $|S_+\rangle$. We isolate the subspace spanned by $\{|T_0(1,1)\rangle, |S_-\rangle,$

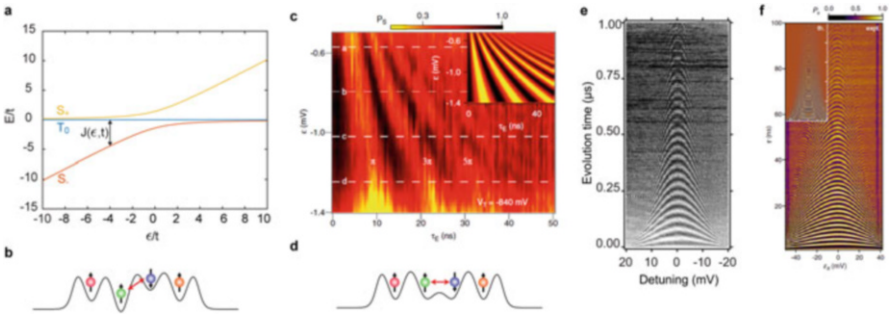

Fig. 2 Exchange coupling in double quantum dots. (**a**) Energies of the effective single-triplet Hamiltonian Eq. (7). The different states and the exchange coupling are labelled. (**b**) Schematic of detuning-controlled exchange oscillations. (**c**) Detuning-controlled exchange oscillations in a GaAs quantum dot. Reprinted from Petta et al., Phyisca E, 35, 2, 251–256 (2006) with the permission of Elsevier. (**d**) Schematic of barrier-controlled exchange oscillations. (**e**) Barrier-controlled exchange oscillations in a Si/SiGe quantum dot. Reed et al., Phys. Rev. Lett., 116, 110402 (2016). Copyright the Authors, licensed under a Creative Commons Attribution (CC BY) license. (**f**) Barrier-controlled exchange oscillations in a GaAs quantum dot. Reprinted with permission from Martins et al., Phys. Rev. Lett, 116, 116801 (2016). Copyright (2016) by the American Physical Society

and $|S_+\rangle\}$. In this basis, and in the absence of magnetic fields, the effective singlet–triplet Hamiltonian is

$$H_{ST} = \begin{pmatrix} 0 & 0 & 0 \\ 0 & \frac{1}{2}\left(\epsilon - \sqrt{\epsilon^2 + 8t^2}\right) & 0 \\ 0 & 0 & \frac{1}{2}\left(\epsilon + \sqrt{\epsilon^2 + 8t^2}\right) \end{pmatrix}. \tag{7}$$

One can see that $|S_-\rangle$ has a lower energy than the $|T_0\rangle$ state. This difference in energy is the exchange coupling $J(\epsilon, t) = \frac{1}{2}\left(\epsilon - \sqrt{\epsilon^2 + 8t^2}\right)$. The energies of this Hamiltonian are shown in Fig. 2a. More detailed methods of calculating exchange couplings in quantum-dot systems involve using the actual eigenfunctions of the quantum-dot confinement potentials through the Heitler–London and Hund–Mulliken approaches [40] and various configuration interaction techniques [41, 42]. These approaches generally rely on a detailed knowledge of the quantum-dot confinement potential.

The previous discussion shows that the two main tools an experimenter has at their disposal to control exchange couplings include the detuning ϵ and the interdot tunnel coupling t (Fig. 2). Historically, exchange couplings in semiconductor quantum dots were manipulated through detuning control [43] (Fig. 2b,c), in part because experimental manipulation of electron states in quantum dots typically requires rapid control of electrochemical potentials, and detuning-controlled exchange oscillations require no extra experimental overhead. A downside to detuning-controlled

exchange coupling is that this method increases the exposure of the spin system to charge noise, and the quality factor of exchange oscillations induced in this way tends to be on the order of 10 [46].

An alternate method to create exchange coupling, which has gained traction in recent years, is to rapidly modify the tunnel barrier between two quantum dots by pulsing the voltage applied to a barrier gate [44, 45] (Fig. 2d–f). This method, called "barrier-controlled," or "symmetric" exchange involves fully separating the electrons into the (1,1) charge configuration and then applying a rapid, positive voltage pulse to the barrier gate. This voltage pulse both lowers the potential barrier between the dots and causes the electron wavefunctions to move closer toward each other [42, 47]. Both effects increase the exchange coupling between electrons. Perhaps most importantly, barrier-controlled exchange coupling is first-order insensitive to charge noise associated with the electrochemical potentials of the dots, leading to significantly improved exchange-oscillation quality factors, at least compared with detuning-controlled exchange.

In principle, both barrier- and detuning-controlled exchange are possible to implement in extended systems of quantum dots. A significant challenge in this regard, however, is that the action of voltages applied to barrier gates modifies not only the tunnel barriers and locations of the dots but also their electrochemical potentials. Likewise, the action of a plunger gate will change not only the electrochemical potential of its associated dot but also all of the other parameters of the confinement potential. The development of "virtual gates" has allowed experimenters to overcome this problem and adjust parameters of quantum-dot spin chains independently [13, 15, 28, 32, 48]. This concept involves measuring how voltages applied to all gates affect all the electrochemical potentials in a system of quantum dots. Assuming that the electrochemical potentials vary linearly with the gate voltages, the exact gate voltages required to create an arbitrary change to the electrochemical potentials may be computed. Recent advances exploiting this concept have demonstrated controlled multiple nonzero exchange couplings in extended arrays of quantum dots [47, 49], as well as charge displacement through multiple quantum dots in series [15]. In addition to the notion of virtual gates, various computer-automated and machine learning tuning approaches have undergone rapid progress in recent years and will no doubt provide a key enabling technology for the exploration of quantum-dot spin chains [27, 32, 34].

3 Quantum Information Processing with Exchange-Coupled Quantum-Dot Spins

Spin qubits based on gate-defined quantum dots are an excellent platform for quantum information processing [20]. Individual electrons can possess extremely long coherence times [50, 51], and semiconductor quantum dots are compatible with advanced semiconductor manufacturing techniques [52, 53]. Exchange coupling

underlies a host of different mechanisms for quantum information processing with semiconductor quantum-dot spin qubits. In this section, we review the different ways in which exchange coupling can facilitate quantum information processing with spins in semiconductor quantum dots.

3.1 Single-Spin Qubits

Conceptually, the simplest spin qubit consists of a single electron, which can either point up or down with respect to an external magnetic field [59] (Fig. 3a). Single-qubit rotations can be driven by applying a real or effective alternating magnetic field perpendicular to the quantizing field. Individual single-spin qubits can have extremely high gate fidelities, far exceeding 99% [50, 60].

A challenge for single-spin qubits, however, is the implementation of a robust multi-qubit operation. The magnetic dipole–dipole coupling between electrons is weak and not usually strong enough to implement high-fidelity two-qubit operations. However, the exchange coupling between two electrons provides a natural route for a two-qubit gate. Specifically, when two spins i and $i + 1$ evolve under exchange J_i for a time $T = \frac{1}{2J_i}$, the exchange coupling generates a SWAP gate (Fig. 4a). Evolution for $\frac{T}{2}$ produces a $\sqrt{\text{SWAP}}$ gate, which can entangle the two electrons. Together with single-qubit gates, a $\sqrt{\text{SWAP}}$ gate is sufficient for universal quantum computing [59, 61, 62]. These facts illustrate on a basic level the potential of exchange coupling for quantum computing and information transfer and motivated initial proposals for quantum computing architectures based on semiconductor quantum dots [55, 59, 63].

In the presence of magnetic gradients between electrons, exchange coupling can enable other two-qubit gates for single spins, such as controlled-phase (CPHASE) (Fig. 4c) or controlled-not (CNOT) (Fig. 4b) gates [64, 65], both of which are also sufficient for universal quantum computing. In spin chains, magnetic gradients are routinely employed to provide single-spin addressability, making the realization of these gates a natural goal [66–69]. The principles of two-qubit gates based on exchange have been experimentally developed in the past decades [43, 50, 61], culminating recently in the demonstration of a CPHASE gate with fidelity exceeding 99%. Such an achievement is a significant milestone for quantum-dot-based quantum information processing [70] because it corroborates the feasibility of operating spin qubits with gate fidelities above the threshold for quantum error correction [71].

Beyond two-qubit gates, exchange coupling can also enable three-qubit operations, such as a Toffoli gate [72] and entangling operations [47].

3.2 *Two-Spin Qubits*

Although the basic spin qubit consists of an individual electron spin, the ability to manipulate exchange opens up the possibility to form new qubits out of multiple-spin states, as shown in Fig. 3. The potential advantage of such a qubit is the possibility of electrical spin-state control [55] and the potential to operate qubits in decoherence-free subspaces [73], which feature long-lived coherence even in the presence of environmental noise.

Perhaps the simplest exchange-enabled multi-spin qubit is the singlet–triplet (ST) qubit [43, 54], formed from two electrons in a double quantum dot (Fig. 3b). The ST qubit Hamiltonian is $H_{ST} = J(\epsilon, t)S_z + \Delta B_z S_x$, in the $\{|S\rangle, |T_0\rangle\}$ subspace, where $J(\epsilon, t)$ is the exchange coupling between the two dots, and ΔB_z is the difference

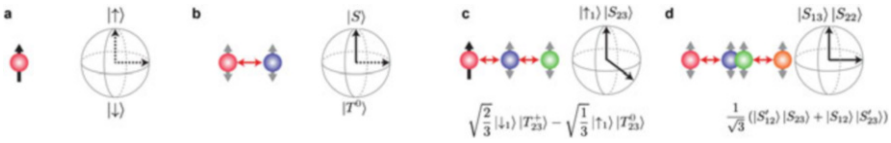

Fig. 3 Comparison between different types of spin qubits. In each panel, the number of spins involved in each qubit is shown. Relevant exchange couplings are highlighted in red, and entangled states are shown with gray arrows. Solid lines on the Bloch sphere indicate exchange-based qubit control axes, and dashed arrows indicate magnetic control axes. (**a**) Single-spin qubit, requiring two magnetic control axes. (**b**) Singlet–triplet qubit, requiring one magnetic control axis [43, 54]. (**c**) Exchange-only qubit with two exchange-based control axes [55]. (**d**) Exchange-only qubit with four (or more electrons) with two orthogonal exchange-based control axes [56–58]. Primed states involve excited levels, such as orbitals or valley states. Reprinted from Kandel et al., App. Phys. Lett., 119,030501 (2021) with the permission of AIP Publishing

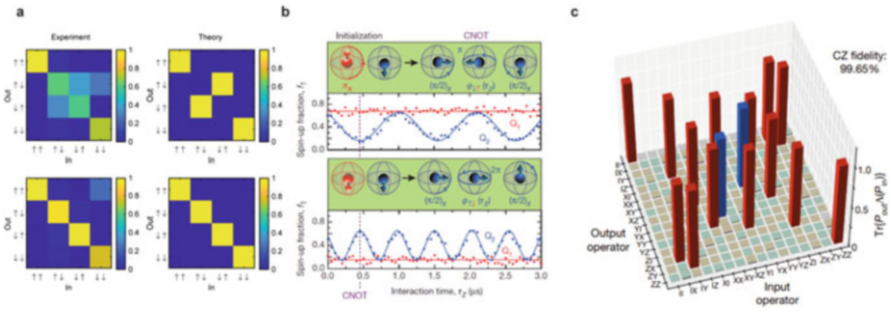

Fig. 4 Exchange coupling in single-spin qubits. (**a**) Top: truth table of a SWAP gate between single spins in GaAs quantum dots driven by exchange. Bottom: truth table of a 2π exchange rotation, from Ref. [61]. (**b**) Evidence for a CNOT gate between single spins in Si/SiO_2 quantum dots driven by exchange. Reprinted with permission from Veldhorst et al., Nature, 526, 410–414 (2015). Copyright Springer Nature (2015). (**c**) Gate-set tomography of a CPHASE gate between single spins in a Si/SiGe quantum well driven by exchange. Xue et al., Nature 601, 343–347 (2022). Copyright the Authors, licensed under a Creative Commons Attribution (CC BY) license

in longitudinal magnetic field between the dots (Fig. 5a). This system occupies a decoherence-free subspace with respect to global magnetic fields that couple to the spin of the electron, because the energies of the $|S\rangle$ and $|T_0\rangle$ states do not depend on the external magnetic field, in contrast to the energies of single-spin states. In addition, the S_z term in H_{ST} depends on electric fields (both ϵ and t depend on electrostatic potentials), which are often easier to generate than pulsed magnetic fields in cryogenic environments. A final benefit of exchange coupling for ST qubits is the possibility of spin-to-charge conversion via the Pauli spin blockade, which enables fast, high-fidelity electrical measurement of spin states [19]. Singlet–triplet qubits, and variations thereof, have been the subject of significant theoretical and experimental research [43, 74, 75, 77–88].

Exchange coupling also enables significant enhancements in the coherence time in ST qubits through dynamical decoupling. Early experiments demonstrated inhomogeneously broadened coherence times of ΔB_z rotations of around 10 ns, due to the fluctuating hyperfine field in GaAs quantum dots [43]. By using dynamical decoupling sequences, with periodic exchange pulses interspersed during the qubit evolution, the coherence time of an ST qubit can be extended to nearly 1 ms [51, 75] (Fig. 5b,c), 4 orders of magnitude larger than the inhomogeneously broadened coherence time.

Exchange coupling also enables two-qubit gates between ST qubits [89–92]. This operation can be intuitively understood in the following picture. Although the ST qubit eigenstates are commonly expressed as the set $\{|S\rangle, |T^0\rangle\}$, an alternative

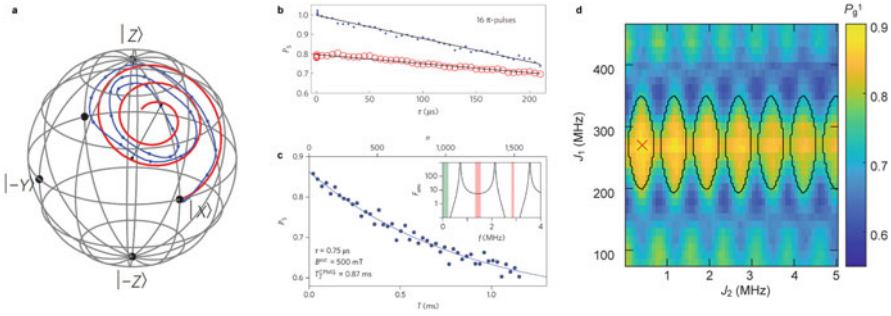

Fig. 5 Exchange coupling in singlet–triplet qubits. (**a**) Exchange coupling, together with controlled magnetic gradients, enables universal quantum control of ST qubits. Reprinted with permission from Foletti et al., Nature Physics, 5, 903–908 (2009). Copyright Springer Nature (2009). (**b**) Exchange coupling also enables decoupling ST qubits from hyperfine noise, extending the coherence time to several hundred μs. Reprinted with permission from Bluhm et al., Nature Physics, 7, 109–113 (2011). Copyright Springer Nature (2011). (**c**) Carefully optimized decoupling pulses can further reduce magnetic fluctuations resulting from the Larmor precession of the individual Ga and As nuclei, resulting in coherence times approaching the millisecond range. Reprinted with permission from Malinowski et al., Nature Nanotechnology, 12, 16–20 (2017). Copyright Springer Nature (2017). (**d**) Evidence of the effective Ising coupling predicted to emerge between exchange-coupled ST qubits. Qiao et al., Nat. Comm., 12, 2142 (2021). Copyright the Authors, licensed under a Creative Commons Attribution (CC BY) license

basis consists of the set $\{|\uparrow\downarrow\rangle, |\downarrow\uparrow\rangle\}$. Considering a chain of four electrons (two ST qubits) with a nonzero exchange coupling between the second and third electrons, one can see that the state $|\uparrow\downarrow\rangle \otimes |\uparrow\downarrow\rangle$ will have a lower energy than the state $|\uparrow\downarrow\rangle \otimes |\downarrow\uparrow\rangle$, which leads to an effective Ising coupling between ST qubits, though care must be taken to prevent leakage. Recently, evidence of this effective Ising coupling has been observed [76] (Fig. 5d).

3.3 *Three-Spin Qubits*

Three electrons in a triple quantum dot create an "exchange-only" qubit [55, 93, 95–99] (Figs. 3d, 6). In contrast to ST qubits, which feature one electrical control axis and one magnetic control axis (single-spin qubits require two magnetic control axes), exchange-only qubits enable complete electrical control, and the two control axes correspond to exchange coupling between the two nearest-neighbor pairs of electrons in the triple dot. The eigenstates of a three-electron exchange-only qubit usually consist of spin states with fixed total spin and triplet- or singlet-like states on one of the outer pairs of spins [55, 93, 96]. In addition to conventional exchange-only qubits, resonant exchange qubits [94, 100] (Fig. 6b) and hybrid qubits [101, 102] leverage exchange couplings to enable control of systems with three electrons [39]. Extending this approach, qubits can also be formed with more than three electrons in three or more quantum dots, and exchange couplings provide complete control over the qubit dynamics [56–58] (Fig. 3d). Such "singlet-only" qubits are predicted to be robust against magnetic field noise. Exchange coupling between triple dots in various configurations can also lead to multi-qubit operations, including CNOT gates [55, 103–105] and CPHASE gates [106].

Since the initial demonstrations by Medford et al. [93, 94] in GaAs quantum dots (Fig. 6a,b), the development of exchange-only qubits has steadily continued,

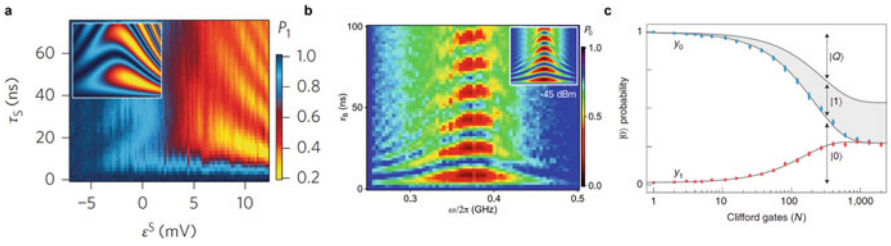

Fig. 6 Exchange coupling in three-electron spin qubits. (**a**) Coherent oscillations in a three-electron exchange only qubit. Reprinted with permission from Medford et al., Nature Nanotechnology, 8, 654–659 (2013). Copyright Springer Nature (2013). (**b**) Rabi oscillations of a resonant-exchange qubit. Reprinted with permission from Medford et al., Phys. Rev. Lett, 111, 050501 (2013). Copyright (2013) by the American Physical Society. (**c**) Randomized benchmarking of an exchange-only qubit. Reprinted with permission from Andrews et al., Nature Nanotechnology, 14, 747–750 (2019). Copyright Springer Nature (2019)

with a recent demonstration of high-fidelity single-qubit gates through randomized benchmarking [95] (Fig. 6c) and advanced device architectures compatible with scaling up systems of exchange-only qubits [53].

4 Quantum Simulation with Quantum-Dot Spin Chains

In addition to uses for quantum information processing, chains of semiconductor quantum dots have great potential for quantum simulation, which is the experimental realization of Hamiltonians that are difficult or impossible to simulate on classical computers, using quantum systems. For example, the Hubbard model, which we discussed above in Sect. 2.3, is a fundamental model of condensed matter physics, and it is thought to underlie phenomena as important as high-temperature superconductivity [107]. In different experimental platforms, especially cold-atom systems [108], simulating the Hubbard phase diagram remains the focus of intense research. While other platforms, like cold-atom systems have made significant progress in understanding different features of the Hubbard model, semiconductor quantum dots also provide an attractive platform in which to study the Hubbard model [109], because they can access parameter regimes not easily accessible to cold-atom systems, including the ultra-low temperature regime. Quantum-dot systems also provide a natural way to study Hubbard physics in solid-state environments. Since the Hubbard model is predicted to underlie important solid-state phenomena, such as high-temperature superconductivity, the study of such models in condensed matter environments seems especially worthwhile.

In another example, the Heisenberg spin chain is predicted to exhibit a host of interesting phenomena, ranging from quantum magnetism [107] and spin chain dynamics [110] to non-equilibrium physics like many-body localization [111]. Semiconductor quantum dots also provide a natural platform in which to explore this model, given the ease of implementing exchange coupling between neighboring spins, together with the capabilities of single-spin control and readout.

In this section, we review recent efforts to explore different aspects of the Hubbard and Heisenberg models. These exciting results show that this is a promising avenue of research, with more exciting results yet to come in the future.

4.1 Charge Physics in the Hubbard Model

Single and double quantum dots are mainstays of semiconductor spin-qubit technology. The tune-up of double quantum-dot systems into the single-charge regime is a routine occurrence in research laboratories throughout the world and the starting point for many quantum-information processing experiments. In some sense, double-quantum-dot systems serve as small-scale simulations of the Hubbard model. For example, the Hubbard model can be used to provide a phenomenological quantum-mechanical description of charge-stability diagrams [113].

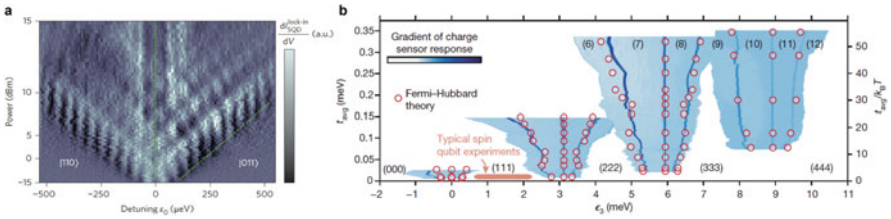

Fig. 7 Quantum simulation of charge physics in the Hubbard model. (**a**) Landau–Zener–Stückelberg interferometry of a single charge tunneling back and forth between distant dots. Reprinted with permission from Braakman et al., Nature Nanotechnology, 8, 432–437 (2013). Copyright Springer Nature (2013). (**b**) Transition from collective to conventional Coulomb blockade in a linear array of three dots. Reprinted with permission from Hensgens et al., Nature, 528, 70–73 (2017). Copyright Springer Nature (2017)

Going beyond double-dot systems, semiconductor quantum dots provide an appealing platform for the simulation of Hubbard physics involved in systems of more than two sites. Early work in this direction was reported by Singha et al. in Ref. [114]. In a GaAs/AlGaAs heterostructure, the authors created an artificial honeycomb lattice by etching the surface of the heterostructure [115]. The resulting pattern created an attractive, periodic potential for electrons, with about 8 electrons per site in an area of about $10^4 \mu m^2$. A characteristic prediction of the Hubbard model for this system is that the on-site energy $\bar{U}$ should scale inversely with the square root of the in-plane magnetic field strength [114]. Inelastic light-scattering experiments revealed both the expected conventional cyclotron mode (with a frequency that scales linearly with the magnetic field), in addition to a mode with the predicted sublinear behavior. This low-frequency mode was taken to represent evidence that Hubbard physics in this artificial honeycomb lattice can be engineered and behaves as expected.

Although such large-scale arrays of quantum dots seem attractive for quantum simulation of many-particle systems [109], recent research has focused on building up such systems one site at a time. In 2013, Braakman et al. presented evidence for the coherent tunneling of an electron between the outer dots of a three-dot linear array [112] (Fig. 7a). Such long-distance coupling between quantum dots can be understood as a second-order tunneling effect within the context of the Hubbard model. The coherence of this tunneling effect was verified through Landau–Zener–Stückleberg interferometry of the charge states near the tunneling transition between the outer dots.

Further exploration of charge physics in the Hubbard model was presented by Hensgens et al. in Ref. [28] (Fig. 7b). The authors studied the transition between individual and collective charge transitions in a series of three quantum dots, as the chemical potentials and tunnel barriers between dots varied. In the limit of high barrier potentials between dots, the three dots acquire charges separately, analogous to a Mott insulating solid. However, when the tunnel barriers are lowered, the three separate dots effectively merge to form a large dot, and the large dot acquires charges one at a time [28].

Although such three-site Hubbard experiments can still be simulated on classical computers without much difficulty, the transition from simulating the Hubbard physics of more than two electrons required significant experimental advances that have set the stage for further developments in this direction. Specifically, an important driver of these results was the ability to tune the chemical potentials and barriers in the linear array simultaneously and independently [13, 15, 28, 32, 48]. This involved establishing a set of virtual plunger and barrier gates, together with computer automated tuning of the device [27, 32, 34]. Such an advance marked an important shift in thinking toward the use of computer automated tuning procedures to aid in the operation of large-scale quantum-dot devices. These advances also paved the way for the exploration of spin effects in the Hubbard and Heisenberg models, as we discuss in the next sections.

4.2 Spin Physics in the Hubbard Model

In addition to charge physics, semiconductor quantum-dot arrays also enable exploring different spin effects in the Hubbard model. The advances described in the previous section focusing on tuning large quantum-dot systems have also translated to advances in the simulation of spin physics in the Hubbard model.

Building on the advances presented by Braakman et al. in Ref. [112], which demonstrated coherent coupling between charge states in distant dots, Baart et al. demonstrated coherent spin interactions between distant dots in Ref. [48]. As discussed above, in the presence of tunnel coupling between two quantum dots (in this case, between the outer dots of a linear three-dot array), one generally expects exchange coupling between spins in those dots to occur. Baart et al. observed evidence for this effect, by initializing and measuring a pair of spins in an outer quantum dot using Pauli spin blockade (Fig. 8a). After allowing the electrons to

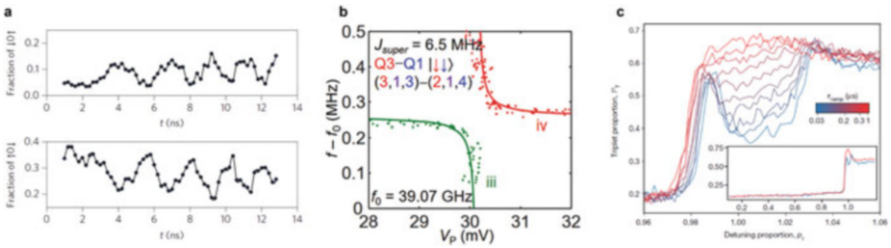

Fig. 8 Quantum simulation of spin physics in the Hubbard model. (**a**) Superexchange between distant electron spins, mediated by an empty quantum dot. Reprinted with permission from Baart et al., Nature Nanotechnology, 12, 26–30 (2017). Copyright Springer Nature (2017). (**b**) Interactions between distant electrons measured in a Si triple dot. Reprinted with permission from Chan et al., Nano Letters, 21, 3, 1517–1522 (2021). Copyright (2021) by the Amperican Chemical Society. (**c**) Signatures of Nagaoka ferromagnetism in a square array of four dots. Reprinted with permission from Deholain et al., Nature 579, 528–533 (2020). Copyright Springer Nature (2020)

evolve when separated, the electrons were recombined and measured via Pauli spin blockade in the same dot. Such an experiment is analogous to experiments demonstrating singlet–triplet exchange oscillations in double quantum dots [43], except that in this case, the electrons were in distant dots.

Similar effects have also been observed in Si triple quantum dots [116] (Fig. 8b), where an effective coupling between electrons in the outer dots of a three-dot array mediated by an occupied quantum dot was observed. By observing how the resonance frequencies of the electron spins in the outer dots changed with detuning, Chan et al. observed an effective nonzero coupling between electrons in the outer two quantum dots.

Collectively, such effects, which create an effective exchange coupling between distant spins, are usually known as superexchange. While many different types of superexchange exist, nearly all rely on virtual excitation of an intermediate entity, such as an empty, singly occupied, or multiply occupied quantum dot. Below, we will discuss superexchange in a spin chain, where an effective coupling between electrons separated by more than one site can be achieved.

A step forward for quantum simulation of spin physics in the Hubbard model in quantum dots occurred with a recent demonstration of Nagaoka ferromagnetism [14]. Working with a 2x2 quantum-dot array [29], Dehollain et al. presented evidence for this phenomenon in Ref. [14]. The theory of Nagaoka [117] provides a prediction for itinerant ferromagnetism in metals for the case of a nearly half-filled band. In the 2x2 quantum-dot array, Dehollain et al. created a nearly half-filled band by filling the array with only three electrons. As in Nagaoka's original theory, the absence of an electron at one of the locations stabilizes the ground state where all of the spins have the same orientation. Experimentally, the system of three electrons was initialized and readout using the Pauli spin blockade associated with a pair of electrons in one dot and an electron with a random spin in another dot. After separating the two electrons in the singlet state via tunneling, the gate voltages were pulsed to different configurations. After allowing the system of three electrons to evolve for a period of time, the researchers measured the system by projecting two of the electrons onto the singlet/triplet basis with a Pauli spin-blockade measurement. The researchers observed an enhanced triplet return probability in the range of gate voltages predicted to demonstrate the ferromagnetic ground state (Fig. 8c).

4.3 Spin Physics in the Heisenberg Model

A special case of the Hubbard model occurs when each site or quantum dot contains only one electron. When the occupancy of each dot remains fixed, the effective Hamiltonian for the spin degrees of freedom can be expressed as the Heisenberg Hamiltonian:

$$H_H = \sum_{i=1}^{N} J_i \mathbf{S}_i \cdot \mathbf{S}_{i+1} + \mathbf{B}_i \cdot \mathbf{S}_i, \tag{8}$$

where $\mathbf{S}_i$ is an operator that corresponds to electron i, and $\mathbf{B}_i$ is the magnetic field experienced by that electron.

In contrast to the Hubbard model, which contains parameters that describe the tunnel couplings and on-site energies, the Heisenberg Hamiltonian involves only the exchange couplings and magnetic fields. While advances in the independent control of chemical potentials have enabled progress in simulating Hubbard physics, the independent control of exchange couplings, which is required to simulate the Heisenberg model, has remained challenging, though recent advances have taken steps toward overcoming this obstacle.

The primary challenge is that exchange couplings depend on both the electrochemical potentials and tunnel couplings. Moreover, tunnel couplings generally depend in a highly nonlinear and nonlocal way on gate voltages [47]. Heuristically, exchange coupling depends on the degree of overlap between electronic wavefunctions, and such overlaps depend sensitively on the barrier potentials and positions of the wavefunctions. A final complication is that when multiple exchange couplings are present, one cannot simply extract the exchange couplings from the measured oscillation frequencies, because the energy gaps in the spectrum of a spin chain do not usually correspond to the bare exchange couplings themselves. These challenges make it difficult to use trial-and-error or interpolation approaches [28–33], which have been used to control tunnel couplings in quantum dots, to modulate exchange couplings.

Qiao et al. overcame this problem and demonstrated coherent exchange coupling between multiple spins in a linear four-dot array. Through a combination of

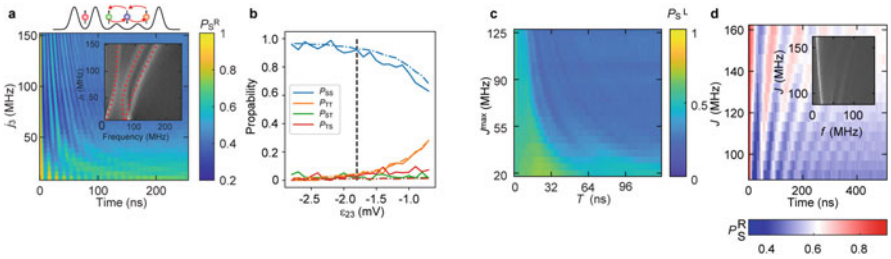

Fig. 9 Quantum simulation of Heisenberg spin chains. (**a**) Coherent multi-spin exchange coupling. Qiao et al., Phys. Rev. X, 10, 031006 (2021). Copyright the Authors, licensed under a Creative Commons Attribution (CC BY) license. (**b**) Preparation of the Heisenberg antiferromagnet. Van Diepen et al., Phys. Rev. X, 11, 041025 (2021). Copyright the Authors, licensed under a Creative Commons Attribution (CC BY) license. (**c**) Adiabatic quantum state transfer. Kandel et al., Nat. Comm. 12, 2156 (2021). Copyright the Authors, licensed under a Creative Commons Attribution (CC BY) license. (**d**) Superexchange between distant electron spins. Reprinted with permission from Qiao et al., Phys. Rev. Lett, 126, 017701 (2021). Copyright (2021) by the American Physical Society

theoretical calculations and electrostatic modeling, they showed that a primary cause of this difficulty is the electronic wavefunction shifts that occur during exchange pulses [42, 47]. For example, during a typical barrier-gate pulse, the electrons on either side of the barrier move closer to or farther away from each other, depending on the sign of the voltage pulse. This motion of the electronic wavefunctions has a significant impact on the magnitude of the exchange coupling. Electrostatic modeling of the potential during a barrier-gate pulse confirmed this picture [47]. Qiao et al. also showed that two models based on the Heitler–London formalism [40, 120] could be used to predict the barrier-gate voltages given a set of desired exchange couplings (Fig. 9a). The model parameters, which describe how much the electrons move in response to voltage pulses, were found by measuring how each of the exchange couplings depended on all of the barrier gate voltages. These models were sufficient to enable the generation of coherent three- and four-spin exchange oscillations within a reasonably wide range of exchange-coupling values [47]. This approach is also extensible to longer arrays of quantum-dot spin qubits.

Van Diepen et al. have also reported the creation of multiple nonzero exchange couplings by adjusting the detunings, instead of the barrier heights, in a linear array of four quantum dots [49]. In addition to demonstrating coherent exchange coupling between all four spins in the array, van Diepen et al. also demonstrated the creation of the ground state of the Heisenberg Hamiltonian, by adiabatically manipulating the exchange couplings beginning from a state composed to two separated singlets (Fig. 9b).

Building on the possibility of precise control of exchange couplings in a quantum-dot array, Kandel et al. demonstrated adiabatic quantum state transfer (AQT) in a chain of four quantum dots [118]. Adiabatic quantum state transfer (AQT), sometimes referred to as adiabatic quantum teleportation [121], is a process that is reminiscent of stimulated Raman adiabatic passage, a time-honored technique from the optical physics community [122]. The basic process of AQT involves a chain of three spins. By starting from a configuration with a strong exchange coupling between two spins, say 2 and 3, and by adiabatically modulating the exchange couplings to a final configuration with a strong coupling between dots 1 and 2, the initial state of dot 1 can be transferred to dot 3, and the joint state of spins 2 and 3 is transferred to dots 1 and 2. Although it has been studied in great detail theoretically over the past decades [121, 123–132], it has only recently been achieved experimentally, despite its great potential for use in quantum information processing experiments.

Kandel et al. implemented AQT in a GaAs/AlGaAs quadruple quantum-dot array [118] (Fig. 9c). To transfer a spin eigenstate from dot 3 to dot 1, a singlet was prepared in dots 1 and 2, by electron exchange with the reservoirs in the presence of large exchange coupling J_1. Then, J_1 was decreased to zero, while J_2 was simultaneously increased. During this process, the spin state of dot 3 was transferred to dot 1, and the singlet state of dots 1 and 2 was transferred to dots 2 and 3. For spin eigenstates, the simulated fidelity of this process in GaAs quantum dots is about 0.95. The simulated fidelity for the transfer of arbitrary quantum states

in GaAs quantum dots is lower, because of the nuclear hyperfine noise. Crucially, the precise fidelity of this operation does not depend on the details of the pulses. This process could also be cascaded to enable long-distance transfer of both single-spin states and spin singlet states.

Another possibility enabled by the ability to independently control exchange couplings in spin chains is long-distance superexchange. As mentioned above, superexchange is an effective coupling between distant spins [110, 133–138], unlike conventional exchange, which only couples nearest-neighbor spins. Generally, superexchange involves an intermediate set of quantum dots that may be empty [139], singly [116], or multiply [140] occupied. One of the most frequently studied systems predicted to exhibit superexchange is a spin chain, consisting of two qubits weakly coupled to the ends of a strongly coupled spin chain [134, 135, 137].

To explore superexchange mediated by a spin chain, Qiao et al. implemented the following Hamiltonian in a system of four quantum dots [119]: $H = j\mathbf{S}_1 \cdot \mathbf{S}_2 + J\mathbf{S}_2 \cdot \mathbf{S}_3 + j\mathbf{S}_3 \cdot \mathbf{S}_4$. When $j \ll J$, superexchange between spins 1 and 4 can occur when spins 2 and 3 have the singlet state, via virtual excitation to the polarized triplet configurations, and at an oscillation frequency of $J' = \frac{j^2}{2J}\left(1 + \frac{3j}{2J}\right)$, up to third order in j (Fig. 9d). If spins 2 and 3 have any of the triplet states, which are nominally degenerate, those spins will evolve in time at a frequency scale of j, and superexchange between the end spins cannot occur with a reasonable fidelity. To realize this scenario, where the chain is prepared as a singlet, Qiao et al. harnessed the AQT process described above to transfer a spin singlet, originally prepared in one of the outer dots, to the interior of the array. After implementing the exchange couplings discussed above, the AQT process was reversed to transfer the end spins to one of the outer pairs of dots, which could be read out with Pauli spin blockade. End-spin oscillations were observed with the expected dependence on the J and j (Fig. 9d).

In addition to pure Heisenberg spin chains, disordered Heisenberg spin chains, [e.g. those with random $\mathbf{B}_i$ in Eq. (8)] are also systems of great interest. Because of the naturally occurring nuclear hyperfine fluctuations, quantum-dot spin qubits enable a straightforward realization of this model. One interesting feature of disordered Heisenberg spin chains is the possibility of many-body localization [111], a phase of matter that seems to violate conventional assumptions about statistical mechanics. In a many-body localized system, despite the presence of interactions, disorder in the system prevents a subset of the system from fully entangling or thermalizing with the rest. The prototypical system thought to exhibit many-body localization is the disordered Heisenberg spin chain. Although many experiments in other platforms have presented evidence for many-body localization [141–145], few have been able to reproduce this seminal model and instead involve longer-range interactions. Because quantum dots enable an exact realization of the disordered Heisenberg spin chain model, semiconductor quantum dots present an attractive platform in which to realize this phenomenon and related effects [12].

The time crystal is another phase of matter that can occur in disordered spin chains [146–150]. In a time crystal, a parent non-thermalizing phase, such as a

many-body localized phase, can stabilize a subharmonic response of the system to a periodic drive indefinitely. The prototypical model for a time crystal is a disordered Ising spin chain. As in the case of many-body localization, the exact realization of this model has evaded implementation, though evidence of phases related to time crystals has been observed in different systems [151–154]. Although disordered Heisenberg spin chains do not enable creating a time crystal [150], it is possible to convert the Heisenberg interaction to an Ising form, through various mechanisms, including magnetic gradients [64, 155] and control pulses [150]. Recent experimental work has suggested that exchange-coupled singlet–triplet qubits can also realize a form of discrete time-crystalline behavior [76, 91]. Although the practical applications of the many-body localized and time-crystal phases are not yet entirely clear, they may be useful in quantum information processing applications as ways to stabilize many-body quantum states [12, 156].

5 Quantum State Transfer in Spin Chains

Some of the features of Heisenberg spin chains we have discussed above, especially superexchange and AQT, have potential applications in quantum computing for the transfer of quantum states between qubits. Transferring quantum information between qubits is essential for quantum error correction [160], and quantum processors with high connectivity can perform more efficiently than those with lower connectivity [161]. Recent years have seen significant progress in this direction. Building on the advances discussed above relating to quantum-dot architectures and fabrication, as well as the independent control of chemical potentials, single electrons can now be shuttled through extended arrays of quantum dots. Mills et al. demonstrated the ability to pump a single charge through an array of nine quantum dots in Si [15]. Depending on the number of charges involved and the repetition rate, this charge pump generated a measurable current that agreed with predictions (Fig. 10a). These experiments demonstrated the high degree of control over charge states afforded by modern quantum-dot architectures.

When electrons move to different dots during tunneling, the spin state of the electron can also be preserved. Initially demonstrated through the preservation of the coherence of a spin singlet during tunneling [43], the preservation of spin coherence has also been demonstrated during tunneling between distant quantum dots [48, 162, 163], in square arrays of quantum dots [157] (Fig. 10b), and in Si quantum dots [164].

One potential drawback to the transfer of spin states through tunneling is that empty quantum dots between the starting and ending locations are required. A route to overcoming this obstacle is to exploit the exchange coupling between neighboring quantum dots. An especially simple way to transfer quantum states with exchange coupling involves pulsed SWAP gates [158]. Although straightforward in concept, this idea had evaded implementation in a system of more than two dots until recently. Kandel et al. demonstrated this approach in a GaAS/AlGaAs quadruple

dot device with overlapping gates, transferring both single-spin eigenstates and entangled states back and forth across the array of four quantum dots through different sequences of SWAP operations [158] (Fig. 10c). Before and after each step, the two pairs of electrons were read out using spin-to-charge conversion techniques associated with Pauli spin blockade [43, 74]. A limiting factor in the previous experiment was the hyperfine interaction between the electron and nuclear spins in the GaAs/AlGaAs heterostructure. As discussed above, the hyperfine-induced dephasing can be minimized by working in Si quantum dots. Sigillito et al. demonstrated the transfer of quantum spin states using "resonant" SWAP gates in the presence of a large magnetic gradient [30] in Si quantum dots. Such gates are generated by an oscillating exchange coupling [80, 83].

An exciting illustration of how exchange coupling can enable long-distance state transfer involves quantum teleportation [165]. Teleportation involves distributing two members of an entangled pair to two experimenters, Alice and Bob. To teleport an unknown qubit state to Bob, Alice should measure the unknown state together

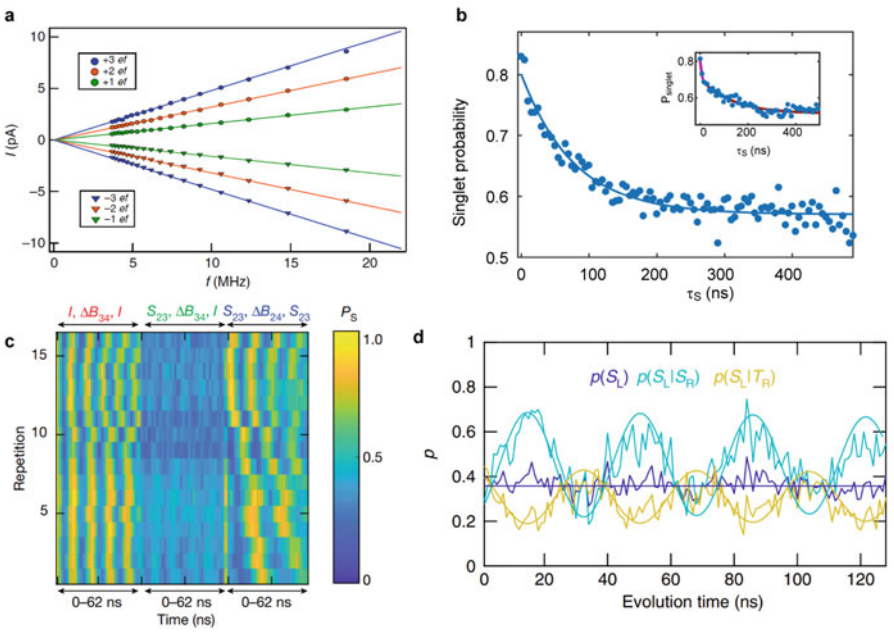

Fig. 10 State transfer in quantum-dot spin chains. (**a**) Current generated by shuttling single electrons through a nine-dot array. Mills et al., Nat. Comm., 10, 1063 (2019) Copyright the Authors, licensed under a Creative Commons Attribution (CC BY) license. (**b**) Motional narrowing of a pair of electron spins shuttled through a square array. Flentje et al., Nat. Comm., 8, 501 (2017). Copyright the Authors, licensed under a Creative Commons Attribution (CC BY) license. (**c**) Entangled state transfer via SWAP operations. Reprinted with permission from Kandel et al., Nature, 573, 553–557 (2019). Copyright Springer Nature (2019). (**d**) Quantum teleportation of entangled states. Qiao et al., Nat. Comm. 11, 3022, (2020). Copyright the Authors, licensed under a Creative Commons Attribution (CC BY) license

with her member of the entangled pair in the Bell-state basis. This measurement projects Bob's member of the entangled pair onto the unknown state, up to a single-qubit rotation that depends on Alice's measurement. Creating the long-distance entangled pair had presented the most challenging obstacle to teleportation in quantum dots [88, 166] and has been the focus of intense research [157, 162, 163]. However, spin-state transfer via Heisenberg exchange [158] solved this challenge. In Ref. [159], Qiao et al. leveraged this advance to perform teleportation in quantum dots (Fig. 10d). To implement teleportation in quantum dots, Qiao et al. created an entangled pair of electrons via Pauli spin blockade in dots 3 and 4 of a four-dot array. The entangled pair was distributed through the array via exchange-based SWAP gates such that it occupied dots 2 and 4. To teleport a state from dot 1 to dot 4, a joint measurement was performed on dots 1 and 2 together via Pauli spin blockade. When this measurement yielded a singlet, which is a maximally entangled Bell state, the state of spin 1 was teleported to spin 4. This procedure was conditional because teleportation occurs only when the measurement of qubits 1–2 yielded a singlet. (A triplet result from this measurement could be any one of the three other Bell states and thus does not provide enough information for complete teleportation.) The experiments of Ref. [159] demonstrated the essence of this procedure by teleporting a classical spin state and entangled states (Fig. 10d).

6 Future Directions and Outlook

In this chapter, we have described the exciting advances and great potential associated with quantum-dot spin chains. In addition to enabling different promising qubits for quantum computing, quantum-dot spin chains also facilitate studying different aspects of the Hubbard and Heisenberg models. In large part, advances along these directions have been driven by parallel developments in the technology of gate-defined semiconductor quantum-dot spin qubits. Today, extended chains of quantum dots can be fabricated and operated with controlled occupancy, and these capabilities directly enable exploring the different features of spin chains that we have described in this chapter.

Despite the significant advances in controlling and exploiting quantum-dot spin chains in recent years, much exciting work remains to be done. On a fundamental level, continuing to understand, model, and predict parameters like tunnel couplings and exchange couplings will continue to drive forward progress in this field. In particular, understanding how to control multiple exchange couplings independently and simultaneously in larger spin chains for many-body quantum simulation or multi-qubit algorithms will create important and exciting opportunities and capabilities for both quantum computing and simulation. It is likely that computer-automated and machine learning approaches [27, 32, 34] for extended quantum-dot systems will become increasingly important.

On the device level, most of the results we have discussed have involved one-dimensional chains. The creation and operation of two-dimensional quantum-dot

arrays [29, 157, 167] is an exciting and active area of research. In addition, the use of materials like Si-based quantum dots [9], which feature lower electron-spin-induced dephasing rates compared with GaAs/AlGaAs quantum dots, may offer new routes to exploring coherent spin phenomena. Further work to understand and minimize effects like charge noise [46, 168, 169] will also become increasingly important.

These expected advances in device design and operation will directly benefit single- and multi-qubit gates driven by exchange. In addition to the theoretical and model-based approaches mentioned above, methods to design and implement noise-resistant exchange pulses [170–172] will likely become increasingly important as gate fidelities and device architectures mature. The possibility of two-dimensional arrays opens up the possibility of efficient error correction schemes [71], as well as dense arrays of qubits with high connectivity [161].

Different multi-spin qubit types also have yet to be experimentally investigated. In general, increasing the number of electrons in multi-spin qubits opens up pathways for reduced sensitivity to noise, at the expense of more complex device designs or control. Whether or not these multi-spin qubits can offer an improvement for quantum computing applications remains to be seen, but they deserve to be explored. In fact, the great variety of potential qubits that can be formed from electrons in quantum dots is one of the unique features of the platform.

As quantum dots continue to mature, new avenues in quantum simulation become available. In particular, it may become possible to explore the Hubbard model in the ultra-low temperature regime [109], where electron–electron interactions are expected to dominate, and which is hypothesized to underlie phenomena like high-temperature superconductivity [109]. Improvements in single-qubit initialization, control, and readout, which will occur through developments in quantum computing, will also benefit simulation efforts.

Besides benefiting from the same technological advances, quantum simulation in spin chains and quantum information processing overlap in the area of long-distance coupling between qubits. We have discussed multiple routes for quantum state transfer, including spin-state transfer via Heisenberg exchange, teleportation, adiabatic state transfer, and superexchange, which exploit some of the unique features of spin chains, mostly in GaAs/AlGaAs quantum dots. The implementation and exploration of these techniques in Si quantum dots, which have longer electron spin coherence times, will be necessary to precisely quantify and benchmark the performance of these techniques and to explore how they might be useful for quantum computing experiments. Although the use of spin chain physics in quantum computing is still in early stages, methods to transfer quantum states between qubits are generally helpful for error correction [160], and it may be that these techniques can enable progress in this direction. In the coming years, it is likely that this exploration will continue and that connections to quantum information science will become stronger and more apparent.

References

1. Y.P. Kandel, H. Qiao, J.M. Nichol, Perspective on exchange-coupled quantum-dot spin chains. Appl. Phys. Lett. **119**, 030501 (2021). https://doi.org/10.1063/5.0055908
2. M. Anderlini, P.J. Lee, B.L. Brown, J. Sebby-Strabley, W.D. Phillips, J.V. Porto, Controlled exchange interaction between pairs of neutral atoms in an optical lattice. Nature **448**, 452 (2007). https://doi.org/10.1038/nature06011
3. Y. He, S.K. Gorman, D. Keith, L. Kranz, J.G. Keizer, M.Y. Simmons, A two-qubit gate between phosphorus donor electrons in silicon. Nature **571**, 371 (2019). https://doi.org/10.1038/s41586-019-1381-2
4. L. Kouwenhoven, C. Marcus, Quantum dots. Physics World **11**(6), 35 (1998). https://doi.org/10.1088/2058-7058/11/6/26
5. L. Kouwenhoven, D.G. Austing, S. Tarucha, Few-electron quantum dots. Rep. Prog. Phys. **64**, 701 (2001). https://stacks.iop.org/0034-4885/64/i=6/a=201
6. W.G. van der Wiel, S. De Franceschi, J.M. Elzerman, T. Fujisawa, S. Tarucha, L.P. Kouwenhoven, Electron transport through double quantum dots. Rev. Mod. Phys. **75**, 1 (2002). https://doi.org/10.1103/RevModPhys.75.1. https://link.aps.org/doi/10.1103/RevModPhys.75.1
7. W.G. van der Wiel, M. Stopa, T. Kodera, T. Hatano, S. Tarucha, Semiconductor quantum dots for electron spin qubits. New J. Phys. **8**(2), 28 (2006). https://doi.org/10.1088/1367-2630/8/2/028
8. R. Hanson, L.P. Kouwenhoven, J.R. Petta, S. Tarucha, L.M.K. Vandersypen, Spins in few-electron quantum dots, Rev. Mod. Phys. **79**, 1217 (2007). https://doi.org/10.1103/RevModPhys.79.1217. https://link.aps.org/doi/10.1103/RevModPhys.79.1217
9. F.A. Zwanenburg, A.S. Dzurak, A. Morello, M.Y. Simmons, L.C.L. Hollenberg, G. Klimeck, S. Rogge, S.N. Coppersmith, M.A. Eriksson, Silicon quantum electronics. Rev. Mod. Phys. **85**, 961 (2013). https://doi.org/10.1103/RevModPhys.85.961
10. G. Scappucci, C. Kloeffel, F.A. Zwanenburg, D. Loss, M. Myronov, J.J. Zhang, S. De Franceschi, G. Katsaros, M. Veldhorst, The germanium quantum information route. Nature Rev. Mater., 1–18 (2020)
11. J.M. Taylor, J.R. Petta, A.C. Johnson, A. Yacoby, C.M. Marcus, M.D. Lukin, Relaxation, dephasing, and quantum control of electron spins in double quantum dots. Phys. Rev. B **76**(3), 035315 (2007). https://doi.org/10.1103/PhysRevB.76.035315
12. E. Barnes, D.L. Deng, R.E. Throckmorton, Y.L. Wu, S. Das Sarma, Noise-induced collective quantum state preservation in spin qubit arrays. Phys. Rev. B **93**, 085420 (2016). https://doi.org/10.1103/PhysRevB.93.085420
13. C. Volk, A.M.J. Zwerver, U. Mukhopadhyay, P.T. Eendebak, C.J. van Diepen, J.P. Dehollain, T. Hensgens, T. Fujita, C. Reichl,W.Wegscheider, L.M.K. Vandersypen, Loading a quantum-dot based "qubyte" register. npj Quantum Inf. **5**, 29 (2019). https://doi.org/10.1038/s41534-019-0146-y
14. J.P. Dehollain, U. Mukhopadhyay, V.P. Michal, Y. Wang, B. Wunsch, C. Reichl, W. Wegscheider, M.S. Rudner, E. Demler, L.M. Vandersypen, Nagaoka ferromagnetism observed in a quantum dot plaquette. Nature **579**, 528 (2020). https://doi.org/10.1038/s41586-020-2051-0
15. A.R. Mills, D.M. Zajac, M.J. Gullans, F.J. Schupp, T.M. Hazard, J.R. Petta, Shuttling a single charge across a one-dimensional array of silicon quantum dots. Nature Communications **10**(1), 1063 (2019). https://doi.org/10.1038/s41467-019-08970-z
16. M. Field, C.G. Smith, M. Pepper, D.A. Ritchie, J.E.F. Frost, G.A.C. Jones, D.G. Hasko, Measurements of coulomb blockade with a noninvasive voltage probe. Phys. Rev. Lett. **70**, 1311 (1993). https://doi.org/10.1103/PhysRevLett.70.1311
17. L. DiCarlo, H.J. Lynch, A.C. Johnson, L.I. Childress, K. Crockett, C.M. Marcus, M.P. Hanson, A.C. Gossard, Differential charge sensing and charge delocalization in a tunable double quantum dot. Phys. Rev. Lett. **92**, 226801 (2004). https://doi.org/10.1103/PhysRevLett.92.226801

18. D.J. Reilly, C.M. Marcus, M.P. Hanson, A.C. Gossard, Fast single-charge sensing with a rf quantum point contact. Appl. Phys. Lett. **91**(16), 162101 (2007). https://doi.org/10.1063/1.2794995
19. C. Barthel, D.J. Reilly, C.M. Marcus, M.P. Hanson, A.C. Gossard, Rapid single-shot measurement of a singlet-triplet qubit. Phys. Rev. Lett. **103**, 160503 (2009). https://doi.org/10.1103/PhysRevLett.103.160503. https://link.aps.org/doi/10.1103/PhysRevLett.103.160503
20. L.M.K. Vandersypen, M.A. Eriksson, Quantum computing with semiconductor spins. Physics Today **72**(8), 38 (2019). https://doi.org/10.1063/PT.3.4270
21. S. Tarucha, D.G. Austing, T. Honda, R.J. van der Hage, L.P. Kouwenhoven, Shell filling and spin effects in a few electron quantum dot. Phys. Rev. Lett. **77**(17), 3613 (1996). https://doi.org/10.1103/PhysRevLett.77.3613. https://link.aps.org/doi/10.1103/PhysRevLett.77.3613
22. L.P. Kouwenhoven, T.H. Oosterkamp, M.W.S. Danoesastro, M. Eto, D.G. Austing, T. Honda, S. Tarucha, Excitation spectra of circular, few-electron quantum dots. Science **278**, 1788 (1997). https://doi.org/10.1126/science.278.5344.1788. https://www.sciencemag.org/content/278/5344/1788.abstract
23. M. Ciorga, A.S. Sachrajda, P. Hawrylak, C. Gould, P. Zawadzki, S. Jullian, Y. Feng, Z. Wasilewski, Addition spectrum of a lateral dot from coulomb and spin-blockade spectroscopy. Phys. Rev. B **61**, R16315 (2000). https://doi.org/10.1103/PhysRevB.61.R16315. https://link.aps.org/doi/10.1103/PhysRevB.61.R16315
24. S.J. Angus, A.J. Ferguson, A.S. Dzurak, R.G. Clark, Gate-defined quantum dots in intrinsic silicon. Nano Lett. **7**, 2051 (2007). https://doi.org/10.1021/nl070949k
25. M.G. Borselli, K. Eng, R.S. Ross, T.M. Hazard, K.S. Holabird, B. Huang, A.A. Kiselev, P.W. Deelman, L.D. Warren, I. Milosavljevic, A.E. Schmitz, M. Sokolich, M.F. Gyure, A.T. Hunter, Undoped accumulation-mode Si/SiGe quantum dots. Nanotechnol. **26**, 375202 (2015). https://doi.org/10.1088/0957-4484/26/37/375202
26. D.M. Zajac, T.M. Hazard, X. Mi, E. Nielsen, J.R. Petta, Scalable gate architecture for a one-dimensional array of semiconductor spin qubits. Phys. Rev. Appl. **6**, 054013 (2016). https://doi.org/10.1103/PhysRevApplied.6.054013
27. T.A. Baart, P.T. Eendebak, C. Reichl, W. Wegscheider, L.M.K. Vandersypen, Computer-automated tuning of semiconductor double quantum dots into the single-electron regime. Appl. Phys. Lett. **108**(21), 213104 (2016). https://doi.org/10.1063/1.4952624
28. T. Hensgens, T. Fujita, L. Janssen, X. Li, C.J. Van Diepen, C. Reichl, W. Wegscheider, S. Das Sarma, L.M.K. Vandersypen, Quantum simulation of a Fermi-Hubbard model using a semiconductor quantum dot array. Nature **548**, 70 EP (2017). https://doi.org/10.1038/nature23022
29. U. Mukhopadhyay, J.P. Dehollain, C. Reichl, W. Wegscheider, L.M.K. Vandersypen, A 2 x 2 quantum dot array with controllable inter-dot tunnel couplings. Appl. Phys. Lett. **112**(18), 183505 (2018). https://doi.org/10.1063/1.5025928
30. A.J. Sigillito, M.J. Gullans, L.F. Edge, M. Borselli, J.R. Petta, Coherent transfer of quantum information in a silicon double quantum dot using resonant swap gates. npj Quantum Inf. **5**(1), 110 (2019). https://doi.org/10.1038/s41534-019-0225-0
31. C.J. van Diepen, P.T. Eendebak, B.T. Buijtendorp, U. Mukhopadhyay, T. Fujita, C. Reichl, W. Wegscheider, L.M.K. Vandersypen, Automated tuning of inter-dot tunnel coupling in double quantum dots. Appl. Phys. Lett. **113**(3), 033101 (2018). https://doi.org/10.1063/1.5031034
32. A.R. Mills, M.M. Feldman, C. Monical, P.J. Lewis, K.W. Larson, A.M. Mounce, J.R. Petta, Computer-automated tuning procedures for semiconductor quantum dot arrays. Appl. Phys. Lett. **115**(11), 113501 (2019). https://doi.org/10.1063/1.5121444
33. T.K. Hsiao, C. van Diepen, U. Mukhopadhyay, C. Reichl, W. Wegscheider, L. Vandersypen, Efficient orthogonal control of tunnel couplings in a quantum dot array. Phys. Rev. Appl. **13**, 054018 (2020). https://doi.org/10.1103/PhysRevApplied.13.054018
34. J.P. Zwolak, T. McJunkin, S.S. Kalantre, J. Dodson, E. MacQuarrie, D. Savage, M. Lagally, S. Coppersmith, M.A. Eriksson, J.M. Taylor, Autotuning of double-dot devices in situ with machine learning. Phys. Rev. Appl. **13**, 034075 (2020). https://doi.org/10.1103/PhysRevApplied.13.034075

35. S.S. Kalantre, J.P. Zwolak, S. Ragole, X. Wu, N.M. Zimmerman, M.D. Stewart, J.M. Taylor, Machine learning techniques for state recognition and auto-tuning in quantum dots. npj Quantum Inf. **5**(1), 6 (2019). https://doi.org/10.1038/s41534-018-0118-7
36. P.A.M. Dirac, R.H. Fowler, On the theory of quantum mechanics. Proc. R. Soc. Lond. A Contain. Papers Math. Phys. Character **112**(762), 661 (1926). https://doi.org/10.1098/rspa.1926.0133
37. W. Heisenberg, Mehrkörperproblem und resonanz in der quantenmechanik. Zeitschrift für Physik **38**(6), 411 (1926). https://doi.org/10.1007/BF01397160
38. N.W. Ashcroft, N.D. Mermin, *Solid State Physics* (Saunders College Publishing, 1976)
39. M. Russ, G. Burkard, Three-electron spin qubits. J. Phys. Condens. Matter **29**(39), 393001 (2017). https://doi.org/10.1088/1361-648x/aa761f
40. G. Burkard, D. Loss, D.P. DiVincenzo, Coupled quantum dots as quantum gates. Phys. Rev. B **59**, 2070 (1999). https://doi.org/10.1103/PhysRevB.59.2070. https://link.aps.org/doi/10.1103/PhysRevB.59.2070
41. E. Nielsen, R.P. Muller, A configuration interaction analysis of exchange in double quantum dots. arXiv:1006.2735 (2010). https://arxiv.org/abs/1006.2735
42. A. Pan, T.E. Keating, M.F. Gyure, E.J. Pritchett, S. Quinn, R.S. Ross, T.D. Ladd, J. Kerckhoff, Resonant exchange operation in triple-quantum-dot qubits for spin–photon transduction. Quantum Sci. Technol. **5**(3), 034005 (2020). https://doi.org/10.1088/2058-9565/ab86c9. https://iopscience.iop.org/article/10.1088/2058-9565/ab86c9
43. J.R. Petta, A.C. Johnson, J.M. Taylor, E. Laird, A. Yacoby, M.D. Lukin, C.M. Marcus, M.P. Hanson, A.C. Gossard, Coherent manipulation of coupled electron spins in semiconductor quantum dots. Science **309**(5744), 2180 (2005). https://doi.org/10.1126/science.1116955
44. M.D. Reed, B.M. Maune, R.W. Andrews, M.G. Borselli, K. Eng, M.P. Jura, A.A. Kiselev, T.D. Ladd, S.T. Merkel, I. Milosavljevic, E.J. Pritchett, M.T. Rakher, R.S. Ross, A.E. Schmitz, A. Smith, J.A. Wright, M.F. Gyure, A.T. Hunter, Reduced sensitivity to charge noise in semiconductor spin qubits via symmetric operation. Phys. Rev. Lett. **116**, 110402 (2016). https://doi.org/10.1103/PhysRevLett.116.110402
45. F. Martins, F.K. Malinowski, P.D. Nissen, E. Barnes, S. Fallahi, G.C. Gardner, M.J. Manfra, C.M. Marcus, F. Kuemmeth, Noise suppression using symmetric exchange gates in spin qubits. Phys. Rev. Lett. **116**, 116801 (2016). https://doi.org/10.1103/PhysRevLett.116.116801
46. O.E. Dial, M.D. Shulman, S.P. Harvey, H. Bluhm, V. Umansky, A. Yacoby, Charge noise spectroscopy using coherent exchange oscillations in a singlet-triplet qubit. Phys. Rev. Lett. **110**, 146804 (2013). https://doi.org/10.1103/PhysRevLett.110.146804. https://link.aps.org/doi/10.1103/PhysRevLett.110.146804
47. H. Qiao, Y.P. Kandel, K. Deng, S. Fallahi, G.C. Gardner, M.J. Manfra, E. Barnes, J.M. Nichol, Coherent multispin exchange coupling in a quantum-dot spin chain. Phys. Rev. X **10**, 031006 (2020). https://doi.org/10.1103/PhysRevX.10.031006
48. T.A. Baart, M. Shafiei, T. Fujita, C. Reichl, W. Wegscheider, L.M.K. Vandersypen, Single-spin CCD. Nature Nanotechnology **11**, 330 (2016). https://doi.org/10.1038/nnano.2015.291
49. C.J. van Diepen, T.K. Hsiao, U. Mukhopadhyay, C. Reichl, W. Wegscheider, L.M.K. Vandersypen. Quantum simulation of antiferromagnetic Heisenberg chain with gate-defined quantum dots. Phys. Rev. X **11**, 041025 (2021). https://doi.org/10.1103/PhysRevX.11.041025
50. M. Veldhorst, J.C.C. Hwang, C.H. Yang, A.W. Leenstra, B. de Ronde, J.P. Dehollain, J.T. Muhonen, F.E. Hudson, K.M. Itoh, A. Morello, A.S. Dzurak, An addressable quantum dot qubit with fault-tolerant control-fidelity. Nature Nanotechnology **9**, 981 (2014). https://doi.org/10.1038/nnano.2014.216
51. F.K. Malinowski, F. Martins, P.D. Nissen, E. Barnes, M.S. Rudner, S. Fallahi, G.C. Gardner, M.J. Manfra, C.M. Marcus, F. Kuemmeth, Notch filtering the nuclear environment of a spin qubit. Nature Nanotechnology **12**, 16–20 (2016). https://doi.org/10.1038/nnano.2016.170
52. A.M.J. Zwerver, T. Krähenmann, T.F. Watson, L. Lampert, H.C. George, R. Pillarisetty, S.A. Bojarski, P. Amin, S.V. Amitonov, J.M. Boter, R. Caudillo, D. Corras-Serrano, J.P. Dehollain, G. Droulers, E.M. Henry, R. Kotlyar, M. Lodari, F. Luthi, D.J. Michalak, B.K. Mueller, S. Neyens, J. Roberts, N. Samkharadze, G. Zheng, O.K. Zietz, G. Scappucci, M. Veldhorst, L.M.K. Vandersypen, J.S. Clarke, Qubits made by advanced semiconductor manufacturing. arXiv:2101.12650 [cond-mat, physics:quant-ph] (2021). https://arxiv.org/abs/2101.12650

53. W. Ha, S.D. Ha, M.D. Choi, Y. Tang, A.E. Schmitz, M.P. Levendorf, K. Lee, T.s. Chappell, J. M. ad Adams, D.R. Hulbert, E. Acuna, R.S. Noah, J.W. Matten, M.P. Jura, J.A. Wright, M.T. Rakher, M.G. Borselli, A flexible design platform for Si/SiGe exchange-only qubits with low disorder. Nano Letters **22**(3), 1443 (2022). https://doi.org/10.1021/acs.nanolett.1c03026
54. J. Levy, Universal quantum computation with spin-1/2 pairs and Heisenberg exchange. Phys. Rev. Lett. **89**(14), 147902 (2002). https://doi.org/10.1103/PhysRevLett.89.147902
55. D.P. DiVincenzo, D. Bacon, J. Kempe, G. Burkard, K.B. Whaley, Universal quantum computation with the exchange interaction. Nature **408**(6810), 339 (2000). https://doi.org/10.1038/35042541
56. A. Sala, J. Danon, Exchange-only singlet-only spin qubit. Phys. Rev. B **95**, 241303 (2017). https://doi.org/10.1103/PhysRevB.95.241303
57. A. Sala, J.H. Qvist, J. Danon, Highly tunable exchange-only singlet-only qubit in a GaAs triple quantum dot. Phys. Rev. Res. **2**, 012062 (2020). https://doi.org/10.1103/PhysRevResearch.2.012062
58. M. Russ, J.R. Petta, G. Burkard, Quadrupolar exchange-only spin qubit. Phys. Rev. Lett. **121**, 177701 (2018). https://doi.org/10.1103/PhysRevLett.121.177701
59. D. Loss, D.P. DiVincenzo, Quantum computation with quantum dots. Phys. Rev. A **57**(1), 120 (1998). https://doi.org/10.1103/PhysRevA.57.120
60. J. Yoneda, K. Takeda, T. Otsuka, T. Nakajima, M.R. Delbecq, G. Allison, T. Honda, T. Kodera, S. Oda, Y. Hoshi, N. Usami, K.M. Itoh, S. Tarucha, A quantum-dot spin qubit with coherence limited by charge noise and fidelity higher than 99.9%. Nature Nanotechnology **13**(2), 102 (2018). https://doi.org/10.1038/s41565-017-0014-x
61. K.C. Nowack, M. Shafiei, M. Laforest, G.E.D.K. Prawiroatmodjo, L.R. Schreiber, C. Reichl, W. Wegscheider, L.M.K. Vandersypen, Single-shot correlations and two-qubit gate of solid-state spins. Science **333**(6047), 1269 (2011). https://doi.org/10.1126/science.1209524
62. R. Brunner, Y.S. Shin, T. Obata, M. Pioro-Ladrière, T. Kubo, K. Yoshida, T. Taniyama, Y. Tokura, S. Tarucha, Two-qubit gate of combined single-spin rotation and interdot spin exchange in a double quantum dot. Phys. Rev. Lett. **107**, 146801 (2011). https://doi.org/10.1103/PhysRevLett.107.146801
63. B.E. Kane, A silicon-based nuclear spin quantum computer. Nature **393**, 133 (1998). https://doi.org/10.1038/30156
64. T. Meunier, V.E. Calado, L.M.K. Vandersypen, Efficient controlled-phase gate for single-spin qubits in quantum dots. Phys. Rev. B **83**, 121403 (2011). https://doi.org/10.1103/PhysRevB.83.121403
65. M. Russ, D.M. Zajac, A.J. Sigillito, F. Borjans, J.M. Taylor, J.R. Petta, G. Burkard, High-fidelity quantum gates in Si/SiGe double quantum dots. Phys. Rev. B **97**, 085421 (2018). https://doi.org/10.1103/PhysRevB.97.085421
66. M. Veldhorst, C.H. Yang, J.C.C. Hwang, W. Huang, J.P. Dehollain, J.T. Muhonen, S. Simmons, A. Laucht, F.E. Hudson, K.M. Itoh, A. Morello, A.S. Dzurak, A two-qubit logic gate in silicon. Nature **526**(7573), 410 (2015). https://doi.org/10.1038/nature15263
67. D.M. Zajac, A.J. Sigillito, M. Russ, F. Borjans, J.M. Taylor, G. Burkard, J.R. Petta, Resonantly driven CNOT gate for electron spins. Science **359**, 439 (2018). https://doi.org/10.1126/science.aao5965
68. T.F. Watson, S.G.J. Philips, E. Kawakami, D.R. Ward, P. Scarlino, M. Veldhorst, D.E. Savage, M.G. Lagally, M. Friesen, S.N. Coppersmith, M.A. Eriksson, L.M.K. Vandersypen, A programmable two-qubit quantum processor in silicon. Nature **555**, 633 (2018). https://doi.org/10.1038/nature25766
69. W. Huang, C.H. Yang, K.W. Chan, T. Tanttu, B. Hensen, R.C.C. Leon, M.A. Fogarty, J.C.C. Hwang, F.E. Hudson, K.M. Itoh, A. Morello, A. Laucht, A.S. Dzurak, Fidelity benchmarks for two-qubit gates in silicon. Nature **569**(7757), 532 (2019). https://doi.org/10.1038/s41586-019-1197-0
70. X. Xue, M. Russ, N. Samkharadze, B. Undseth, A. Sammak, G. Scappucci, L.M.K. Vandersypen, Computing with spin qubits at the surface code error threshold. Nature **601**, 343 (2022). https://doi.org/10.1038/s41586-021-04273-w

71. A.G. Fowler, M. Mariantoni, J.M. Martinis, A.N. Cleland, Surface codes: Towards practical large-scale quantum computation. Phys. Rev. A **86**, 032324 (2012). https://doi.org/10.1103/PhysRevA.86.032324. https://link.aps.org/doi/10.1103/PhysRevA.86.032324
72. M.J. Gullans, J.R. Petta, Protocol for a resonantly driven three-qubit Toffoli gate with silicon spin qubits. Phys. Rev. B **100**, 085419 (2019). https://doi.org/10.1103/PhysRevB.100.085419
73. D. Bacon, J. Kempe, D.A. Lidar, K.B. Whaley, Universal fault-tolerant quantum computation on decoherence-free subspaces. Phys. Rev. Lett. **85**, 1758 (2000). https://doi.org/10.1103/PhysRevLett.85.1758. https://link.aps.org/doi/10.1103/PhysRevLett.85.1758
74. S. Foletti, H. Bluhm, D. Mahalu, V. Umansky, A. Yacoby, Universal quantum control of two-electron spin quantum bits using dynamic nuclear polarization. Nature Physics **5**(12), 903 (2009). https://doi.org/10.1038/nphys1424
75. H. Bluhm, S. Foletti, I. Neder, M.S. Rudner, D. Mahalu, V. Umansky, A. Yacoby, Dephasing time of GaAs electron-spin qubits coupled to a nuclear bath exceeding 200 μs. Nature Physics **7**(2), 109 (2010). https://doi.org/10.1038/nphys1856
76. H. Qiao, Y.P. Kandel, J.S.V. Dyke, S. Fallahi, G.C. Gardner, M.J. Manfra, E. Barnes, J.M. Nichol, Floquet-enhanced spin swaps. Nature Communications **12**(1), 2142 (2021). https://doi.org/10.1038/s41467-021-22415-6
77. H. Bluhm, S. Foletti, D. Mahalu, V. Umansky, A. Yacoby, Enhancing the coherence of a spin qubit by operating it as a feedback loop that controls its nuclear spin bath. Phys. Rev. Lett. **105**(21), 216803 (2010). https://doi.org/10.1103/PhysRevLett.105.216803
78. M.D. Shulman, O.E. Dial, S.P. Harvey, H. Bluhm, V. Umansky, A. Yacoby, Demonstration of entanglement of electrostatically coupled singlet-triplet qubits. Science **336**(6078), 202 (2012). https://doi.org/10.1126/science.1217692
79. B.M. Maune, M.G. Borselli, B. Huang, T.D. Ladd, P.W. Deelman, K.S. Holabird, A.A. Kiselev, I. Alvarado-Rodriguez, R.S. Ross, A.E. Schmitz, M. Sokolich, C.A. Watson, M.F. Gyure, A.T. Hunter, Coherent singlet-triplet oscillations in a silicon-based double quantum dot. Nature **481**(7381), 344 (2012). https://doi.org/10.1038/nature10707
80. M.D. Shulman, S.P. Harvey, J.M. Nichol, S.D. Bartlett, A.C. Doherty, V. Umansky, A. Yacoby, Suppressing qubit dephasing using real-time Hamiltonian estimation. Nature Communications **5**(May), 5156 (2014). https://doi.org/10.1038/ncomms6156
81. X. Wu, D.R. Ward, J.R. Prance, D. Kim, J.K. Gamble, R.T. Mohr, Z. Shi, D.E. Savage, M.G. Lagally, M. Friesen, S.N. Coppersmith, M.A. Eriksson, Two-axis control of a singlet—triplet qubit with an integrated micromagnet. Proc. Natl. Acad. Sci. **111**(33), 11938 (2014). https://doi.org/10.1073/pnas.1412230111
82. J.M. Nichol, S.P. Harvey, M.D. Shulman, A. Pal, V. Umansky, E.I. Rashba, B.I. Halperin, A. Yacoby, Quenching of dynamic nuclear polarization by spin-orbit coupling in GaAs quantum dots. Nature Communications **6**, 7682 (2015). https://doi.org/10.1038/ncomms8682
83. J..M. Nichol, L.A. Orona, S.P. Harvey, S. Fallahi, G.C. Gardner, M.J. Manfra, A. Yacoby, High-fidelity entangling gate for double-quantum-dot spin qubits. npj Quantum Inf. **3**(1), 3 (2017). https://doi.org/10.1038/s41534-016-0003-1
84. A. Noiri, T. Nakajima, J. Yoneda, M.R. Delbecq, P. Stano, T. Otsuka, K. Takeda, S. Amaha, G. Allison, K. Kawasaki, Y. Kojima, A. Ludwig, A.D. Wieck, D. Loss, S. Tarucha, A fast quantum interface between different spin qubit encodings. Nature Communications **9**(1), 5066 (2018). https://doi.org/10.1038/s41467-018-07522-1
85. P. Harvey-Collard, N.T. Jacobson, C. Bureau-Oxton, R.M. Jock, V. Srinivasa, A.M. Mounce, D.R. Ward, J.M. Anderson, R.P. Manginell, J.R. Wendt, T. Pluym, M.P. Lilly, D.R. Luhman, M. Pioro-Ladrière, M.S. Carroll, Spin-orbit interactions for singlet-triplet qubits in silicon. Phys. Rev. Lett. **122**, 217702 (2019). https://doi.org/10.1103/PhysRevLett.122.217702
86. M.A. Fogarty, K.W. Chan, B. Hensen, W. Huang, T. Tanttu, C.H. Yang, A. Laucht, M. Veldhorst, F.E. Hudson, K.M. Itoh, D. Culcer, T.D. Ladd, A. Morello, A.S. Dzurak, Integrated silicon qubit platform with single-spin addressability, exchange control and singleshot singlet-triplet readout. Nature Communications **9**(1), 4370 (2018). https://doi.org/10.1038/s41467-018-06039-x

87. P. Cerfontaine, T. Botzem, J. Ritzmann, S.S. Humpohl, A. Ludwig, D. Schuh, D. Bougeard, A.D. Wieck, H. Bluhm, Closed-loop control of a GaAs-based singlet-triplet spin qubit with 99.5% gate fidelity and low leakage. Nature Communications **11**(1), 1 (2020). https://doi.org/10.1038/s41467-020-17865-3
P. Cerfontaine, T. Botzem, J. Ritzmann, S.S. Humpohl, A. Ludwig, D. Schuh, D. Bougeard, A.D. Wieck, H. Bluhm, Closed-loop control of a GaAs-based singlet-triplet spin qubit with 99.5% gate fidelity and low leakage. Nature Communications **11**(1), 1 (2020)
88. K. Takeda, A. Noiri, J. Yoneda, T. Nakajima, S. Tarucha, Resonantly driven singlet-triplet spin qubit in silicon. Phys. Rev. Lett. **124**, 117701 (2020). https://doi.org/10.1103/PhysRevLett.124.117701
89. J. Klinovaja, D. Stepanenko, B.I. Halperin, D. Loss, Exchange-based CNOT gates for singlet-triplet qubits with spin-orbit interaction. Phys. Rev. B **86**, 085423 (2012). https://link.aps.org/doi/10.1103/PhysRevB.86.085423
90. R. Li, X. Hu, J.Q. You, Controllable exchange coupling between two singlet-triplet qubits. Phys. Rev. B **86**, 205306 (2012). https://doi.org/10.1103/PhysRevB.86.205306
91. M.P. Wardrop, A.C. Doherty, Exchange-based two-qubit gate for singlet-triplet qubits. Phys. Rev. B **90**, 045418 (2014). https://doi.org/10.1103/PhysRevB.90.045418
92. P. Cerfontaine, R. Otten, M.A. Wolfe, P. Bethke, H. Bluhm, High-fidelity gate set for exchange-coupled singlet-triplet qubits. Phys. Rev. B **101**, 155311 (2020). https://doi.org/10.1103/PhysRevB.101.155311. https://link.aps.org/doi/10.1103/PhysRevB.101.155311
93. J. Medford, J. Beil, J.M. Taylor, S.D. Bartlett, A.C. Doherty, E.I. Rashba, D.P. DiVincenzo, H. Lu, A.C. Gossard, C.M. Marcus, Self-consistent measurement and state tomography of an exchange-only spin qubit. Nature Nanotechnology **8**, 654 (2013). https://doi.org/10.1038/nnano.2013.168
94. J. Medford, J. Beil, J.M. Taylor, E.I. Rashba, H. Lu, A.C. Gossard, C.M. Marcus, Quantum-dot-based resonant exchange qubit. Phys. Rev. Lett. **111**, 050501 (2013). https://doi.org/10.1103/PhysRevLett.111.050501
95. R.W. Andrews, C. Jones, M.D. Reed, A.M. Jones, S.D. Ha, M.P. Jura, J. Kerckhoff, M. Levendorf, S. Meenehan, S.T. Merkel, A. Smith, B. Sun, A.J. Weinstein, M.T. Rakher, T.D. Ladd, M.G. Borselli, Quantifying error and leakage in an encoded Si/SiGe triple-dot qubit. Nature Nanotechnology **14**(8), 747 (2019). https://doi.org/10.1038/s41565-019-0500-4
96. E.A. Laird, J.M. Taylor, D.P. DiVincenzo, C.M. Marcus, M.P. Hanson, A.C. Gossard, Coherent spin manipulation in an exchange-only qubit. Phys. Rev. B **82**, 075403 (2010). https://doi.org/10.1103/PhysRevB.82.075403
97. L. Gaudreau, G. Granger, A. Kam, G.C. Aers, S.A. Studenikin, P. Zawadzki, M. Pioro-Ladriere, Z.R. Wasilewski, A.S. Sachrajda, Coherent control of three-spin states in a triple quantum dot. Nature Physics **8**, 54 (2012). https://doi.org/10.1038/nphys2149
98. K. Eng, T.D. Ladd, A. Smith, M.G. Borselli, A.A. Kiselev, B.H. Fong, K.S. Holabird, T.M. Hazard, B. Huang, P.W. Deelman, I. Milosavljevic, A.E. Schmitz, R.S. Ross, M.F. Gyure, A.T. Hunter, Isotopically enhanced triple-quantum-dot qubit. Sci. Adv. **1**, 1500214 (2015). https://doi.org/10.1126/sciadv.1500214. https://advances.sciencemag.org/content/1/4/e1500214
99. Y.P. Shim, C. Tahan, Charge-noise-insensitive gate operations for always-on, exchange-only qubits. Phys. Rev. B **93**, 121410 (2016). https://doi.org/10.1103/PhysRevB.93.121410
100. F.K. Malinowski, F. Martins, P.D. Nissen, S. Fallahi, G.C. Gardner, M.J. Manfra, C.M. Marcus, F. Kuemmeth, Symmetric operation of the resonant exchange qubit. Phys. Rev. B **96**, 045443 (2017). https://doi.org/10.1103/PhysRevB.96.045443
101. Z. Shi, C.B. Simmons, J.R. Prance, J.K. Gamble, T.S. Koh, Y.P. Shim, X. Hu, D.E. Savage, M.G. Lagally, M.A. Eriksson, M. Friesen, S.N. Coppersmith, Fast hybrid silicon double-quantum-dot qubit. Phys. Rev. Lett. **108**, 140503 (2012). https://doi.org/10.1103/PhysRevLett.108.140503
102. D. Kim, Z. Shi, C.B. Simmons, D.R. Ward, J.R. Prance, T.S. Koh, J.K. Gamble, D.E. Savage, M.G. Lagally, M. Friesen, S.N. Coppersmith, M.A. Eriksson, Quantum control and process tomography of a semiconductor quantum dot hybrid qubit. Nature **511**(7507), 70 (2014). https://doi.org/10.1038/nature13407

103. B.H. Fong, S.M. Wandzura, Universal quantum computation and leakage reduction in the 3-qubit decoherence free subsystem. Quantum Inf. Comput. **11**(11-12) 1003–1018 (2011)
104. F. Setiawan, H.Y. Hui, J.P. Kestner, X. Wang, S.D. Sarma, Robust two-qubit gates for exchange-coupled qubits. Phys. Rev. B **89**, 085314 (2014). https://doi.org/10.1103/PhysRevB.89.085314. https://link.aps.org/doi/10.1103/PhysRevB.89.085314
105. M.P. Wardrop, A.C. Doherty, Characterization of an exchange-based two-qubit gate for resonant exchange qubits. Phys. Rev. B **93**, 075436 (2016). https://doi.org/10.1103/PhysRevB.93.075436. https://link.aps.org/doi/10.1103/PhysRevB.93.075436
106. D. Zeuch, R. Cipri, N.E. Bonesteel, Analytic pulse-sequence construction for exchange-only quantum computation. Phys. Rev. B **90**, 045306 (2014). https://doi.org/10.1103/PhysRevB.90.045306. https://link.aps.org/doi/10.1103/PhysRevB.90.045306
107. A. Auerbach, *Interacting electrons and quantum magnetism* (Springer Science & Business Media, 2012)
108. L. Tarruell, L. Sanchez-Palencia, Quantum simulation of the Hubbard model with ultracold fermions in optical lattices. Comptes Rendus Physique **19**(6), 365 (2018). https://doi.org/10.1016/j.crhy.2018.10.013
109. P. Barthelemy, L.M.K. Vandersypen, Quantum dot systems: a versatile platform for quantum simulations. Annalen der Physik **525**(10-11), 808 (2013). https://doi.org/10.1002/andp.201300124
110. S. Bose, Quantum communication through spin chain dynamics: an introductory overview. Contemporary Physics **48**(1), 13 (2007). https://doi.org/10.1080/00107510701342313
111. A. Pal, D.A. Huse, Many-body localization phase transition. Phys. Rev. B **82**, 174411 (2010). https://doi.org/10.1103/PhysRevB.82.174411
112. F.R. Braakman, P. Barthelemy, C. Reichl, W. Wegscheider, L.M.K. Vandersypen, Long-distance coherent coupling in a quantum dot array. Nature Nanotechnology **8**, 432 (2013). https://doi.org/10.1038/nnano.2013.67
113. X. Wang, S. Yang, S. Das Sarma, Quantum theory of the charge-stability diagram of semiconductor double-quantum-dot systems. Phys. Rev. B **84**, 115301 (2011). https://doi.org/10.1103/PhysRevB.84.115301. https://link.aps.org/doi/10.1103/PhysRevB.84.115301
114. A. Singha, M. Gibertini, B. Karmakar, S. Yuan, M. Polini, G. Vignale, M. Katsnelson, A. Pinczuk, L. Pfeiffer, K. West, et al., Two-dimensional Mott-Hubbard electrons in an artificial honeycomb lattice. Science **332**(6034), 1176 (2011). https://doi.org/10.1126/science.1204333
115. M. Gibertini, A. Singha, V. Pellegrini, M. Polini, G. Vignale, A. Pinczuk, L.N. Pfeiffer, K.W. West, Engineering artificial graphene in a two-dimensional electron gas. Phys. Rev. B **79**, 241406 (2009). https://doi.org/10.1103/PhysRevB.79.241406. https://link.aps.org/doi/10.1103/PhysRevB.79.241406
116. K.W. Chan, H. Sahasrabudhe, W. Huang, Y. Wang, H.C. Yang, M. Veldhorst, J.C.C. Hwang, F.A. Mohiyaddin, F.E. Hudson, K.M. Itoh, A. Saraiva, A. Morello, A. Laucht, R. Rahman, A.S. Dzurak, Exchange coupling in a linear chain of three quantum-dot spin qubits in silicon. Nano Letters **21**(3), 1517–1522 (2020). https://doi.org/10.1021/acs.nanolett.0c04771
117. Y. Nagaoka, Ferromagnetism in a narrow, almost half-filled *s* band. Phys. Rev. **147**, 392 (1966). https://doi.org/10.1103/PhysRev.147.392. https://link.aps.org/doi/10.1103/PhysRev.147.392
118. Y.P. Kandel, H. Qiao, S. Fallahi, G.C. Gardner, M.J. Manfra, J.M. Nichol, Adiabatic quantum state transfer in a semiconductor quantum-dot spin chain. Nature Communications **12**(1), 2156 (2021). https://doi.org/10.1038/s41467-021-22416-5
119. H. Qiao, Y.P. Kandel, S. Fallahi, G.C. Gardner, M.J. Manfra, X. Hu, J.M. Nichol, Long-distance superexchange between semiconductor quantum-dot electron spins. Phys. Rev. Lett. **126**, 017701 (2021). https://doi.org/10.1103/PhysRevLett.126.017701
120. R. de Sousa, X. Hu, S. Das Sarma, Effect of an inhomogeneous external magnetic field on a quantum-dot quantum computer. Phys. Rev. A **64**, 042307 (2001). https://doi.org/10.1103/PhysRevA.64.042307
121. D. Bacon, S.T. Flammia, Adiabatic gate teleportation. Phys. Rev. Lett. **103**, 120504 (2009). https://doi.org/10.1103/PhysRevLett.103.120504

122. N.V. Vitanov, A.A. Rangelov, B.W. Shore, K. Bergmann, Stimulated Raman adiabatic passage in physics, chemistry, and beyond. Rev. Mod. Phys. **89**, 015006 (2017). https://doi.org/10.1103/RevModPhys.89.015006
123. E. Farhi, J. Goldstone, S. Gutmann, M. Sipser, Quantum computation by adiabatic evolution, arXiv:quant-ph/0001106 (2000). https://doi.org/10.48550/arXiv.quant-ph/0001106
124. A.D. Greentree, J.H. Cole, A.R. Hamilton, L.C.L. Hollenberg, Coherent electronic transfer in quantum dot systems using adiabatic passage. Phys. Rev. B **70**, 235317 (2004). https://doi.org/10.1103/PhysRevB.70.235317
125. V. Srinivasa, J. Levy, C.S. Hellberg, Flying spin qubits: A method for encoding and transporting qubits within a dimerized Heisenberg spin-$\frac{1}{2}$ chain. Phys. Rev. B **76**, 094411 (2007). https://doi.org/10.1103/PhysRevB.76.094411
126. D. Petrosyan, G.M. Nikolopoulos, P. Lambropoulos, State transfer in static and dynamic spin chains with disorder. Phys. Rev. A **81**, 042307 (2010). https://doi.org/10.1103/PhysRevA.81.042307
127. N. Chancellor, S. Haas, Using theJ1–j2quantum spin chain as an adiabatic quantum data bus. New J. Phys. **14**(9), 095025 (2012). https://doi.org/10.1088/1367-2630/14/9/095025
128. S. Oh, Y.P. Shim, J. Fei, M. Friesen, X. Hu, Resonant adiabatic passage with three qubits. Phys. Rev. A **87**, 022332 (2013). https://doi.org/10.1103/PhysRevA.87.022332
129. U. Farooq, A. Bayat, S. Mancini, S. Bose, Adiabatic many-body state preparation and information transfer in quantum dot arrays. Phys. Rev. B **91**, 134303 (2015). https://doi.org/10.1103/PhysRevB.91.134303
130. R. Menchon-Enrich, A. Benseny, V. Ahufinger, A.D. Greentree, T. Busch, J. Mompart, Reports on progress in physics spatial adiabatic passage: A review of recent progress related content. Rep. Prog. Phys. **79**, 074401 (2016). https://doi.org/10.1088/0034-4885/79/7/074401
131. Y. Ban, X. Chen, S. Kohler, G. Platero, Spin entangled state transfer in quantum dot arrays: Coherent adiabatic and speed-up protocols. Adv. Quantum Tech. **2**(10) (2019). https://doi.org/10.1002/qute.201900048
132. M.J. Gullans, J.R. Petta, Coherent transport of spin by adiabatic passage in quantum dot arrays. Phys. Rev. B **102**, 155404 (2020). https://doi.org/10.1103/PhysRevB.102.155404
133. S. Bose, Quantum communication through an unmodulated spin chain. Phys. Rev. Lett. **91**, 207901 (2003). https://doi.org/10.1103/PhysRevLett.91.207901
134. A. Wójcik, T. Łuczak, P. Kurzyński, A. Grudka, T. Gdala, M. Bednarska, Unmodulated spin chains as universal quantum wires. Phys. Rev. A **72**, 034303 (2005). https://doi.org/10.1103/PhysRevA.72.034303
135. L. Campos Venuti, C. Degli Esposti Boschi, M. Roncaglia, Long-distance entanglement in spin systems. Phys. Rev. Lett. **96**, 247206 (2006). https://doi.org/10.1103/PhysRevLett.96.247206
136. M. Friesen, A. Biswas, X. Hu, D. Lidar, Efficient multiqubit entanglement via a spin bus. Phys. Rev. Lett. **98**, 230503 (2007). https://doi.org/10.1103/PhysRevLett.98.230503
137. S. Oh, M. Friesen, X. Hu, Even-odd effects of heisenberg chains on long-range interaction and entanglement. Phys. Rev. B **82**, 140403 (2010). https://doi.org/10.1103/PhysRevB.82.140403
138. S. Oh, L.A. Wu, Y.P. Shim, J. Fei, M. Friesen, X. Hu, Heisenberg spin bus as a robust transmission line for quantum-state transfer. Phys. Rev. A **84**, 022330 (2011). https://doi.org/10.1103/PhysRevA.84.022330
139. T.A. Baart, T. Fujita, C. Reichl, W. Wegscheider, L.M.K. Vandersypen, Coherent spin-exchange via a quantum mediator. Nature Nanotechnology **12**, 26 (2016). https://doi.org/10.1038/nnano.2016.188
140. F.K. Malinowski, F. Martins, T.B. Smith, S.D. Bartlett, A.C. Doherty, P.D. Nissen, S. Fallahi, G.C. Gardner, M.J. Manfra, C.M. Marcus, F. Kuemmeth, Fast spin exchange across a multielectron mediator. Nature Communications **10**(1), 1196 (2019). https://doi.org/10.1038/s41467-019-09194-x

141. M. Schreiber, S.S. Hodgman, P. Bordia, H.P. Lüschen, M.H. Fischer, R. Vosk, E. Altman, U. Schneider, I. Bloch, Observation of many-body localization of interacting fermions in a quasirandom optical lattice. Science **349**(6250), 842 (2015). https://doi.org/10.1126/science.aaa7432
142. J.y. Choi, S. Hild, J. Zeiher, P. Schauß, A. Rubio-Abadal, T. Yefsah, V. Khemani, D.A. Huse, I. Bloch, C. Gross, Exploring the many-body localization transition in two dimensions. Science **352**(6293), 1547 (2016). https://doi.org/10.1126/science.aaf8834
143. S.S. Kondov, W.R. McGehee, W. Xu, B. DeMarco, Disorder-induced localization in a strongly correlated atomic Hubbard gas. Phys. Rev. Lett. **114**, 083002 (2015). https://doi.org/10.1103/PhysRevLett.114.083002
144. J. Smith, A. Lee, P. Richerme, B. Neyenhuis, P.W. Hess, P. Hauke, M. Heyl, D.A. Huse, C. Monroe, Many-body localization in a quantum simulator with programmable random disorder. Nature Physics **12**(10), 907 (2016). https://doi.org/10.1038/nphys3783
145. K.X. Wei, C. Ramanathan, P. Cappellaro, Exploring localization in nuclear spin chains. Phys. Rev. Lett. **120**, 070501 (2018). https://doi.org/10.1103/PhysRevLett.120.070501
146. V. Khemani, A. Lazarides, R. Moessner, S.L. Sondhi, Phase structure of driven quantum systems. Phys. Rev. Lett. **116**, 250401 (2016). https://doi.org/10.1103/PhysRevLett.116.250401
147. D.V. Else, B. Bauer, C. Nayak, Floquet time crystals. Phys. Rev. Lett. **117**, 090402 (2016). https://doi.org/10.1103/PhysRevLett.117.090402
148. C.W. von Keyserlingk, S.L. Sondhi, Phase structure of one-dimensional interacting Floquet systems. II. symmetry-broken phases. Phys. Rev. B **93**, 245146 (2016). https://doi.org/10.1103/PhysRevB.93.245146
149. N.Y. Yao, A.C. Potter, I.D. Potirniche, A. Vishwanath, Discrete time crystals: Rigidity, criticality, and realizations. Phys. Rev. Lett. **118**, 030401 (2017). https://doi.org/10.1103/PhysRevLett.118.030401
150. E. Barnes, J.M. Nichol, S.E. Economou, Stabilization and manipulation of multispin states in quantum-dot time crystals with heisenberg interactions. Phys. Rev. B **99**, 035311 (2019). https://doi.org/10.1103/PhysRevB.99.035311
151. J. Zhang, P.W. Hess, A. Kyprianidis, P. Becker, A. Lee, J. Smith, G. Pagano, I.D. Potirniche, A.C. Potter, A. Vishwanath, N.Y. Yao, C. Monroe, Observation of a discrete time crystal. Nature **543**(7644), 217 (2017). https://doi.org/10.1038/nature21413
152. S. Choi, J. Choi, R. Landig, G. Kucsko, H. Zhou, J. Isoya, F. Jelezko, S. Onoda, H. Sumiya, V. Khemani, C. von Keyserlingk, N.Y. Yao, E. Demler, M.D. Lukin, Observation of discrete time-crystalline order in a disordered dipolar many-body system. Nature **543**(7644), 221 (2017). https://doi.org/10.1038/nature21426
153. J. Rovny, R.L. Blum, S.E. Barrett, Observation of discrete-time-crystal signatures in an ordered dipolar many-body system. Phys. Rev. Lett. **120**, 180603 (2018). https://doi.org/10.1103/PhysRevLett.120.180603
154. S. Pal, N. Nishad, T.S. Mahesh, G.J. Sreejith, Temporal order in periodically driven spins in star-shaped clusters. Phys. Rev. Lett. **120**, 180602 (2018). https://doi.org/10.1103/PhysRevLett.120.180602
155. B. Li, J.S. Van Dyke, A. Warren, S.E. Economou, E. Barnes, Discrete time crystal in the gradient-field heisenberg model. Phys. Rev. B **101**, 115303 (2020). https://doi.org/10.1103/PhysRevB.101.115303
156. J.S. Van Dyke, Y.P. Kandel, H. Qiao, J.M. Nichol, S.E. Economou, E. Barnes, Protecting quantum information in quantum dot spin chains by driving exchange interactions periodically. Phys. Rev. B **103**, 245303 (2021). https://doi.org/10.1103/PhysRevB.103.245303
157. H. Flentje, P.A. Mortemousque, R. Thalineau, A. Ludwig, A.D. Wieck, C. Bäuerle, T. Meunier, Coherent long-distance displacement of individual electron spins. Nature Communications **8**(1), 501 (2017)
158. Y.P. Kandel, H. Qiao, S. Fallahi, G.C. Gardner, M.J. Manfra, J.M. Nichol, Coherent spin-state transfer via heisenberg exchange. Nature **573**(7775), 553 (2019). https://doi.org/10.1038/s41586-019-1566-8

159. H. Qiao, Y.P. Kandel, S.K. Manikandan, A.N. Jordan, S. Fallahi, G.C. Gardner, M.J. Manfra, J.M. Nichol, Conditional teleportation of quantum-dot spin states. Nature Communications **11**(1), 3022 (2020). https://doi.org/10.1038/s41467-020-16745-0
160. A.G. Fowler, C.D. Hill, L.C.L. Hollenberg, Quantum-error correction on linear-nearest-neighbor qubit arrays. Phys. Rev. A **69**, 042314 (2004). https://doi.org/10.1103/PhysRevA.69.042314
161. N.M. Linke, D. Maslov, M. Roetteler, S. Debnath, C. Figgatt, K.A. Landsman, K. Wright, C. Monroe, Experimental comparison of two quantum computing architectures. Proc. Natl. Acad. Sci. **114**(13), 3305 (2017). https://doi.org/10.1073/pnas.1618020114
162. T. Fujita, T.A. Baart, C. Reichl, W. Wegscheider, L.M.K. Vandersypen, Coherent shuttle of electron-spin states. npj Quantum Inf. **3**(1), 22 (2017). https://doi.org/10.1038/s41534-017-0024-4
163. T. Nakajima, M.R. Delbecq, T. Otsuka, S. Amaha, J. Yoneda, A. Noiri, K. Takeda, G. Allison, A. Ludwig, A.D. Wieck, X. Hu, F. Nori, S. Tarucha, Coherent transfer of electron spin correlations assisted by dephasing noise. Nature Communications **9**(1), 2133 (2018). https://doi.org/10.1038/s41467-018-04544-7
164. J. Yoneda, W. Huang, M. Feng, C.H. Yang, K.W. Chan, T. Tanttu, W. Gilbert, R. Leon, F. Hudson, K. Itoh, et al., Coherent spin qubit transport in silicon. Nature Communications **12**(1), 1 (2021). https://doi.org/10.1038/s41467-021-24371-7
165. C.H. Bennett, G. Brassard, C. Crépeau, R. Jozsa, A. Peres, W.K. Wootters, Teleporting an unknown quantum state via dual classical and Einstein-Podolsky-Rosen channels. Phys. Rev. Lett. **70**, 1895 (1993). https://doi.org/10.1103/PhysRevLett.70.1895
166. R.L. de Visser, M. Blaauboer, Deterministic teleportation of electrons in a quantum dot nanostructure. Phys. Rev. Lett. **96**, 246801 (2006). https://doi.org/10.1103/PhysRevLett.96.246801
167. P.A. Mortemousque, E. Chanrion, B. Jadot, H. Flentje, A. Ludwig, A.D. Wieck, M. Urdampilleta, C. Bäuerle, T. Meunier, Coherent control of individual electron spins in a two-dimensional quantum dot array. Nature Nanotechnology **16**(3), 296 (2021). https://doi.org/10.1038/s41565-020-00816-w
168. E.J. Connors, J. Nelson, H. Qiao, L.F. Edge, J.M. Nichol, Low-frequency charge noise in Si/SiGe quantum dots. Phys. Rev. B **100**, 165305 (2019). https://doi.org/10.1103/PhysRevB.100.165305
169. E.J. Connors, J. Nelson, J.M. Nichol. Charge-noise spectroscopy of Si/SiGe quantum dots via dynamically-decoupled exchange oscillations, Nature Communications **13**, 940 (2022). https://doi.org/10.1038/s41467-022-28519-x
170. X. Wang, L.S. Bishop, J.P. Kestner, E. Barnes, K. Sun, S. Das Sarma, Composite pulses for robust universal control of singlet-triplet qubits. Nature Communications **3**, 997 (2012). https://doi.org/10.1038/ncomms2003
171. J.P. Kestner, X. Wang, L.S. Bishop, E. Barnes, S. Das Sarma, Noise-resistant control for a spin qubit array. Phys. Rev. Lett. **110**, 140502 (2013). https://doi.org/10.1103/PhysRevLett.110.140502. https://link.aps.org/doi/10.1103/PhysRevLett.110.140502
172. G.T. Hickman, X. Wang, J.P. Kestner, S. Das Sarma, Dynamically corrected gates for an exchange-only qubit. Phys. Rev. B **88**, 161303 (2013). https://doi.org/10.1103/PhysRevB.88.161303. https://link.aps.org/doi/10.1103/PhysRevB.88.161303